Computational geomechanics of the thawing and freezing frozen soils

Steve WaiChing Sun, Columbia University

Acknowledgments

Hyoung Suk Suh
PhD graduate &
Postdoc

SeonHong Na
PhD graduate, now
assistant professor at
McMaster University

Qing Yin
Postdoc, now
Research Engineer at
Apple

Motivation: climate change and energy demand

- **NCA: average annual temperatures in Alaska are projected to rise by 2°F to 4°F by 2050**

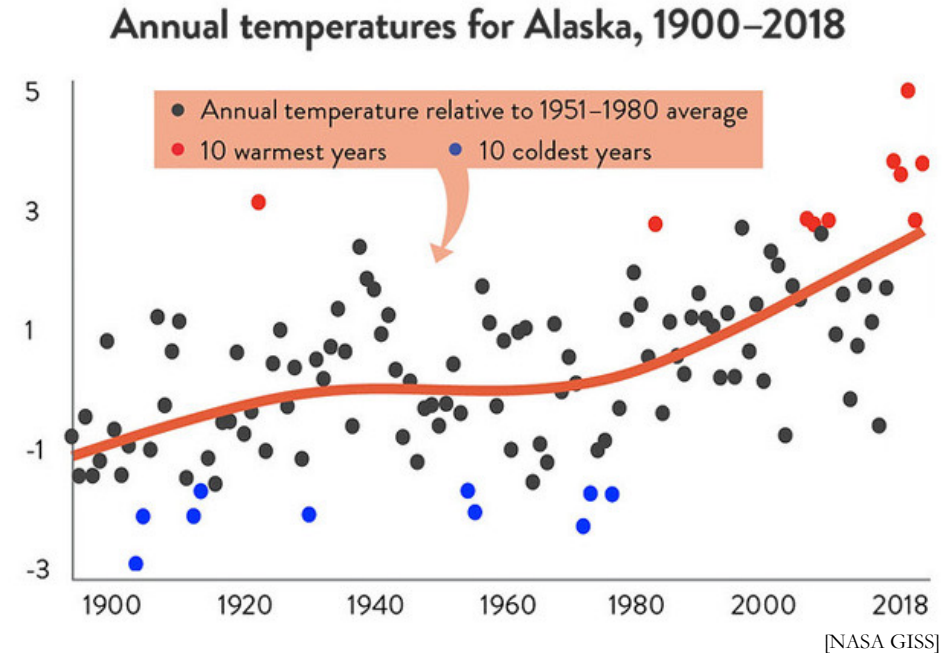

[NASA GISS]

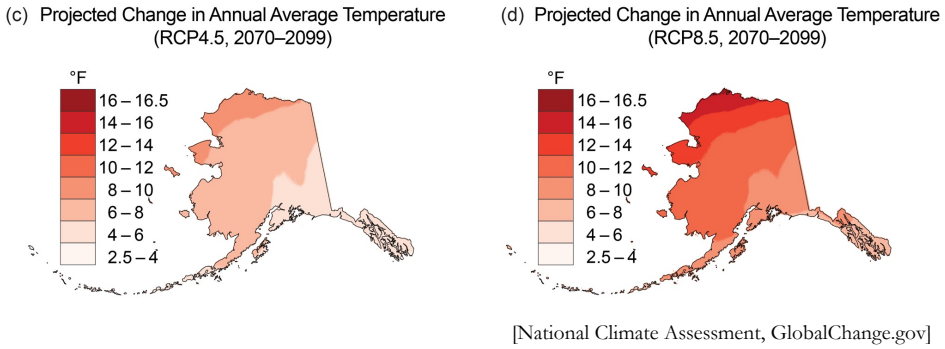

[National Climate Assessment, GlobalChange.gov]

Motivation: climate change and energy demand

- EIA projects nearly **50% rise** in world energy usage by 2050, led by the growth of non-OECD regions

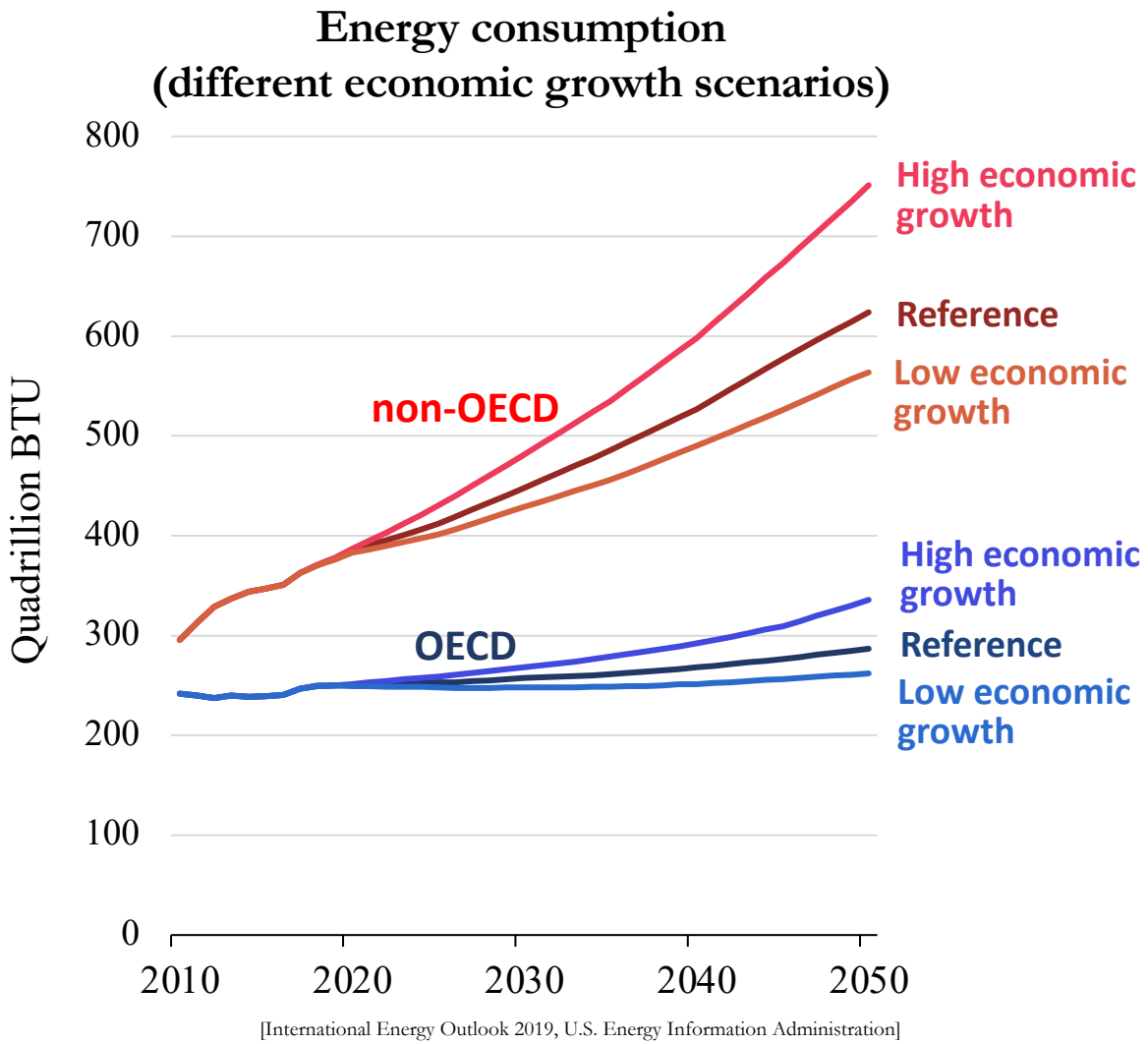

[International Energy Outlook 2019, U.S. Energy Information Administration]

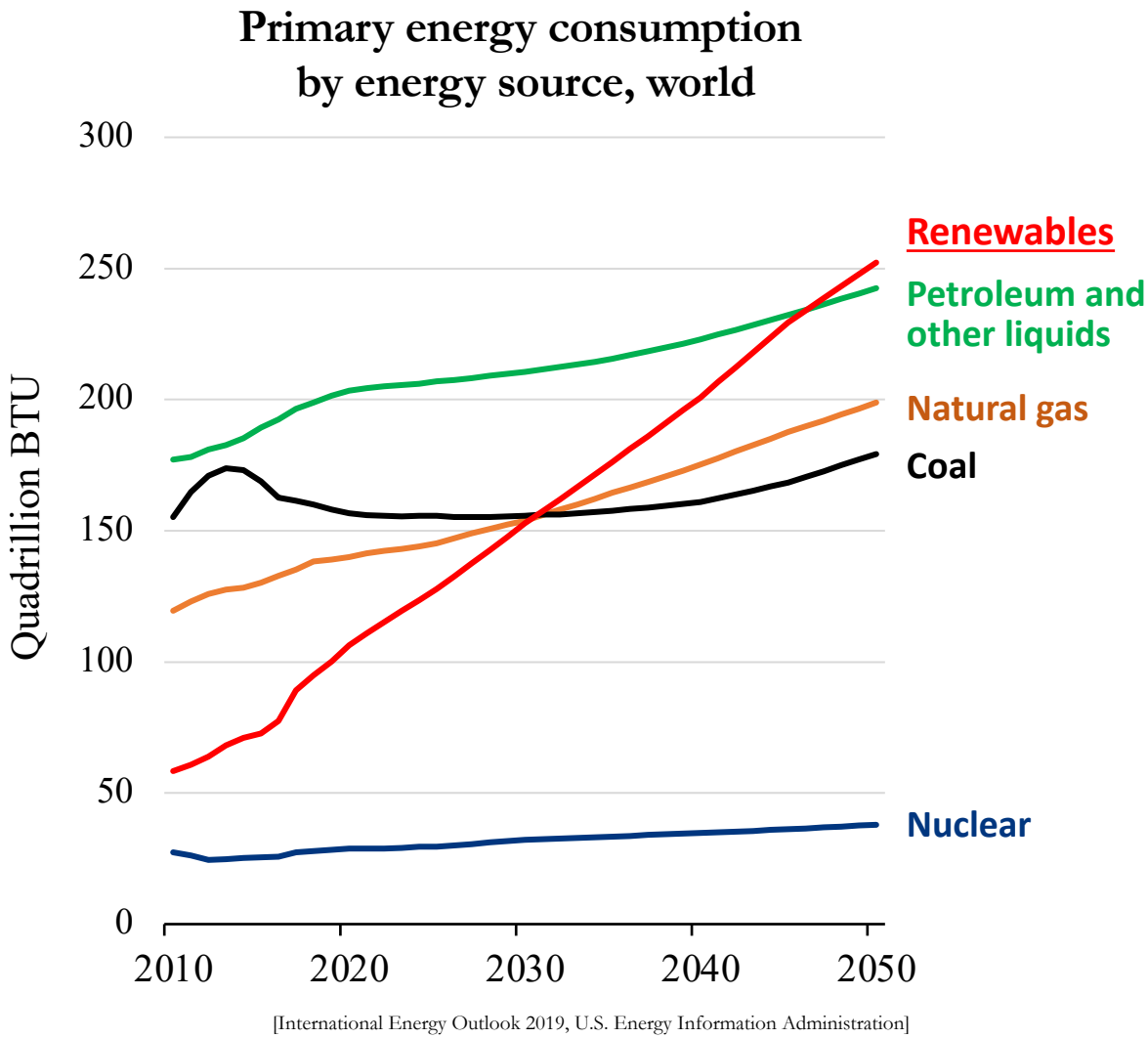

[International Energy Outlook 2019, U.S. Energy Information Administration]

Motivation: Engineering applications

Artificial ground freezing

Freeze-thaw damage

Understanding Frozen porous media is important for

1. ground freezing technique (for construction, sealing contaminated (e.g. Fukushima Daiichi nuclear power plant).
2. Freeze-thaw damage of pavement under the influence of changing climate.

Motivation: Engineering applications

➢ Porous Media (Geomaterials – frozen soil.)

- In northern climate areas (or permafrost area)
  - Mechanical volume expansion of pore water: frost heaving
  - Changes of climate lead to substantial temperature increase: (instability of structures, freeze-thaw actions, etc.)
  - Pavement damage, under ground pipeline damage

<Pavement damage>

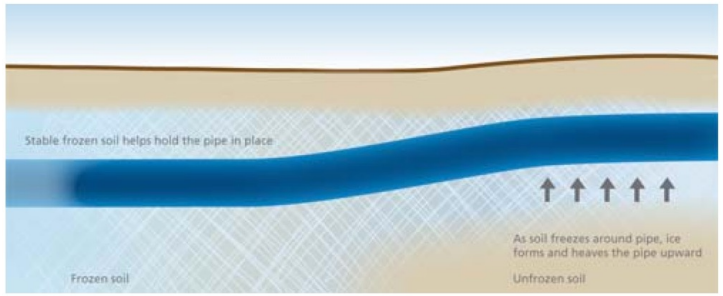

<Frost Heave>

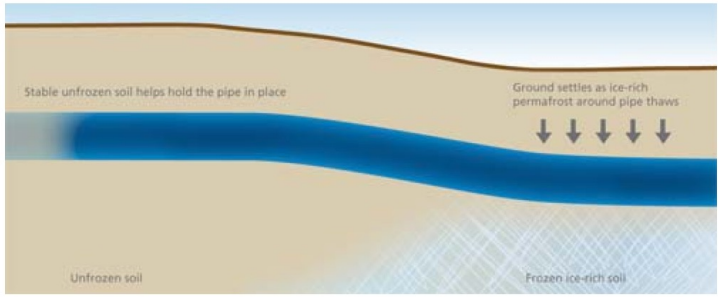

<Thawing Settlement>

https://www.neb-one.gc.ca/pplctnflng/mjrpp/archive/mcknzgs/rfd/rfdv1p3-eng.html

Motivation: Preparation for climate changes

ALEC LUHN SCIENCE 10.20.16 7:00 AM

ARCTIC CITIES CRUMBLE AS CLIMATE CHANGE THAWS PERMAFROST

A man walks past a Soviet era housing block near the Nurd Kamal mosque in the arctic Russian city of Norilsk.
ROGER BACON/REUTERS/ALAMY

This story originally appeared on the Guardian and is part of the Climate Desk collaboration.

From Wired Magazine, Oct 20th

Motivation: Crack forms within the shear band during thawing

Frozen soil specimen at the end of the undrained triaxial compression test (LEFT), immediately exposed to the room temperature (MIDDLE) and after 8 minutes at room temperature (RIGHT).

Freezing-induced anisotropy in freezing clayey soil

Frozen soil as a three-phase material

- Premelting dynamics theory explains the physics of freezing phenomenon in porous media (Rempel, et al. 2004, Wettlaufer & Worster 2006)
- Soils are hydrophilic and prefer contacting unfrozen water rather than ice
- Interfacial premelting separating ice from solid skeleton.
- Cryo-suction effect is well explained.

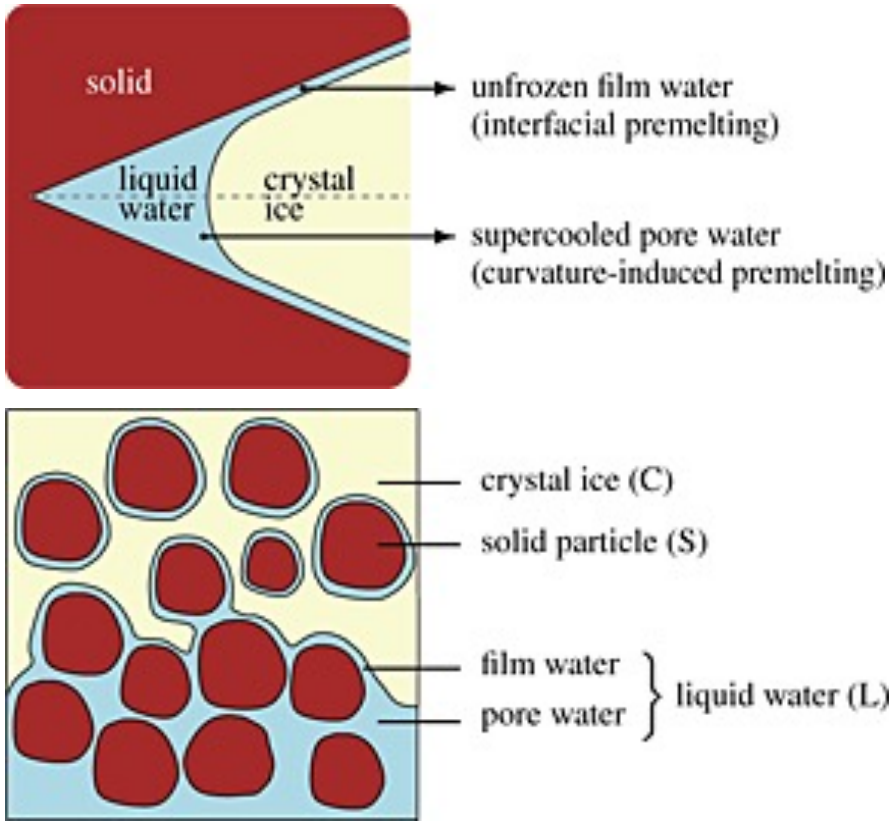

Multi-phase decomposition

- Consider porous media with porosity ϕ
- The pores are saturated with the mixture of ice (C) and water (L).

$$\phi = \frac{V_{\mathrm{C}} + V_{\mathrm{L}}}{V}$$

- Degree of saturations for liquid water and ice:

$$S_{\mathrm{L}} = \frac{V_{\mathrm{L}}}{V_{\mathrm{C}} + V_{\mathrm{L}}}, S_{\mathrm{C}} = 1 - S_{\mathrm{L}}$$

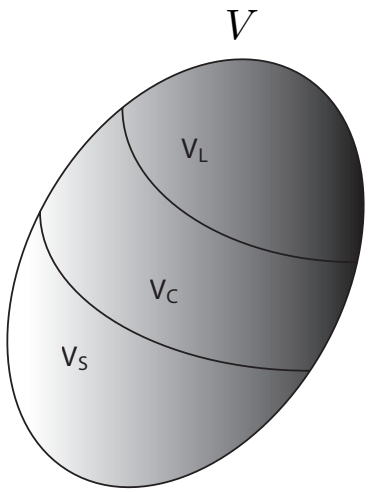

Representative volume element

X-ray tomographic experiments in freezing soil

- Experimental study shows the anisotropic deformation of frozen soil (Amato et al. 2021).
- Two potential reasons:
  - Cryo-suction effect. Water flows from unfrozen to the frozen region.
  - Preferred direction of ice growth.
- Transverse isotropy depends on the growth of ice.

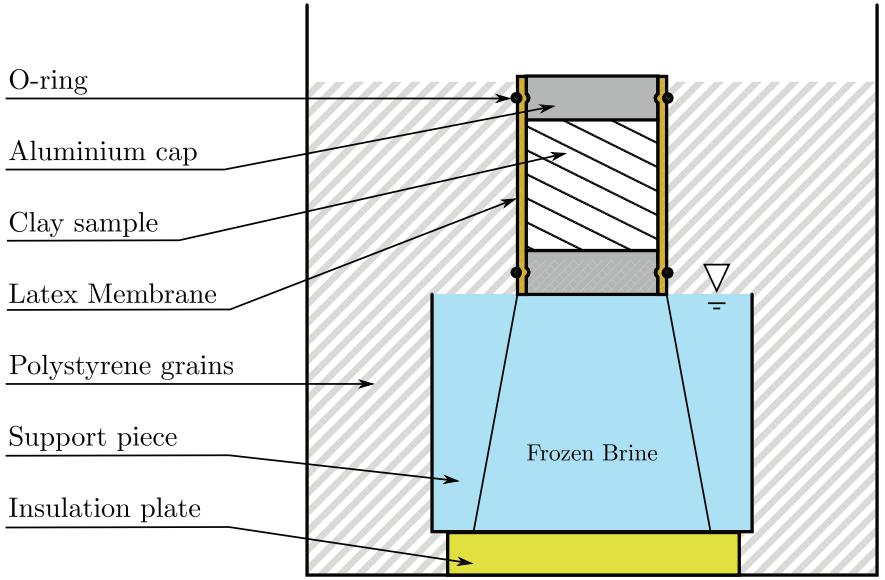

Experimental setup

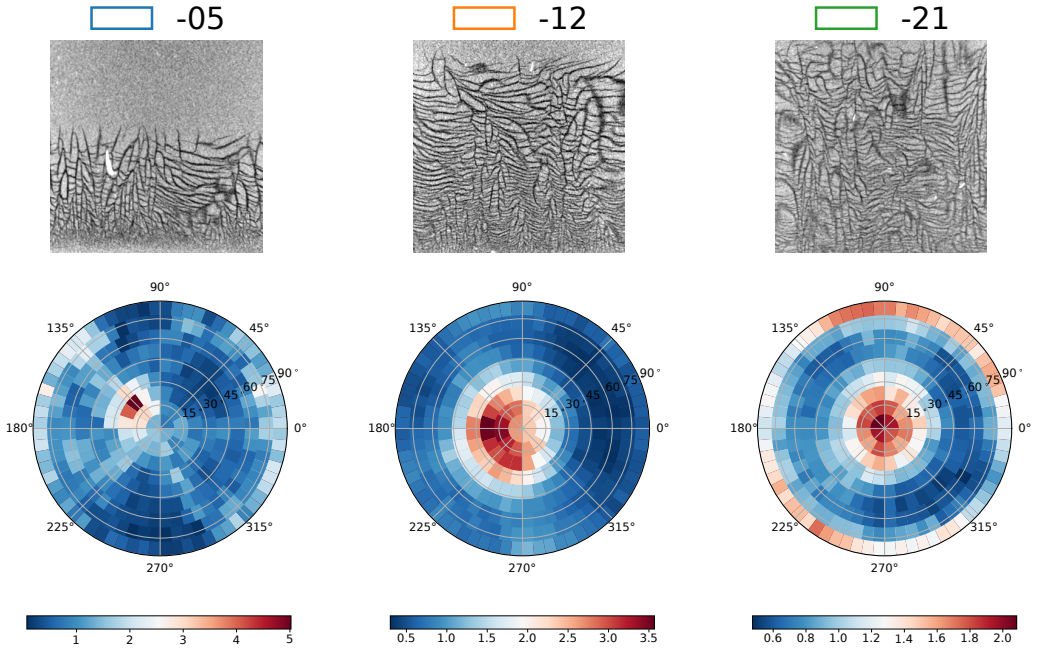

Distribution of ice fringe orientations

Fully coupled thermal-hydro-mechanical approach

Three fields to solve – Temperature, water pressure, and displacement

Three governing equations

Component-based PDE for THM problems

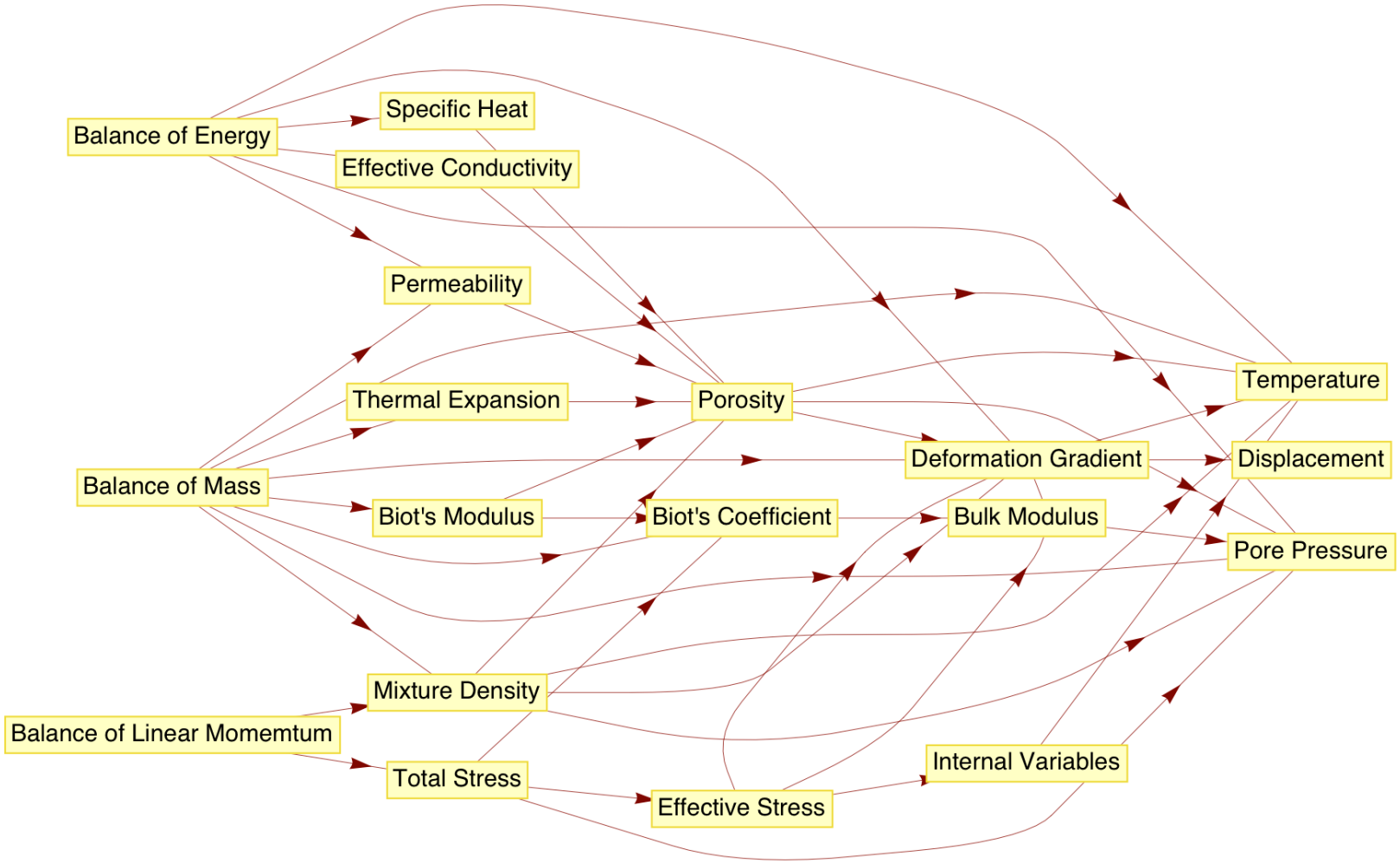

- The computer model can be considered as a mathematical object called directed graph.
- Each vertex represent a physical quality
- Each edge represents a mapping or function that links the upstream and downstream physical qualities (vertices)

Sun, IJNME 2015

Balance of mass

$$\frac{\mathrm{d}^{\mathrm{S}}\rho^{\mathrm{S}}}{\mathrm{d}t} + \rho^{\mathrm{S}}\,\nabla\cdot\boldsymbol{v}_{\mathrm{S}} = 0$$

$$\frac{\mathrm{d}^{\mathrm{L}}\rho^{\mathrm{L}}}{\mathrm{d}t} + \rho^{\mathrm{L}}\,\nabla\cdot\boldsymbol{v}_{\mathrm{L}} = -\dot{m}_{\mathrm{L}\to\mathrm{C}}$$

$$\frac{\mathrm{d}^{\mathrm{C}}\rho^{\mathrm{C}}}{\mathrm{d}t} + \rho^{\mathrm{C}}\,\nabla\cdot\boldsymbol{v}_{\mathrm{C}} = \dot{m}_{\mathrm{L}\to\mathrm{C}} \longrightarrow$$

Rate of phase transition from liquid to ice.

$$\rho_{\mathrm{L}}[\phi\dot{S}_{\mathrm{L}} + S_{\mathrm{L}}\nabla\cdot\boldsymbol{v}_{\mathrm{S}}] + \rho_{\mathrm{C}}[\phi\dot{S}_{\mathrm{C}} + S_{\mathrm{C}}\nabla\cdot\boldsymbol{v}_{\mathrm{S}}] + \nabla\cdot[\rho_{\mathrm{L}}(\phi\tilde{\boldsymbol{v}}_{\mathrm{L}} - \phi s_{\mathrm{T}}\nabla T)] = 0$$

Displacement related

Pressure, temperature related

Soret effect

Balance of energy

$$c_{\mathrm{F}}\dot{T} = -\nabla \cdot \boldsymbol{q}_{\mathrm{T}} + \frac{\phi S_{\mathrm{L}} c_{\mathrm{FL}}}{\rho_{\mathrm{L}}} \rho_{\mathrm{L}} (\phi \tilde{\boldsymbol{v}}_{\mathrm{L}} - \phi s_{\mathrm{T}} \nabla T) \cdot \nabla T + D_{\mathrm{mech}} + R_{\mathrm{T}}$$

Specific heat

Heat conduction

Heat convection

Mechanical dissipation

$$c_{\mathrm{F}} = c_{\mathrm{FS}}\phi^{\mathrm{S}} + c_{\mathrm{FL}}\phi^{\mathrm{L}} + c_{\mathrm{FC}}\phi^{\mathrm{C}} + \rho_{\mathrm{C}}\phi l \frac{\partial S_{\mathrm{L}}}{\partial T}$$

Effect of latent heat (Na and Sun 2017)

$$D_{\mathrm{mech}} = \beta \boldsymbol{\sigma}' : \boldsymbol{\varepsilon}^{\mathrm{p}}$$

Balance of linear momentum

- Bishop's effective theory (Bishop 1959)

$$\nabla \cdot \boldsymbol{\sigma}' + \rho \boldsymbol{g} = 0$$

$$\boldsymbol{\sigma}' = \boldsymbol{\sigma} + \bar{p}\boldsymbol{I}, \text{ with } \bar{p} = S_{\mathrm{L}} p_{\mathrm{L}} + S_{\mathrm{C}} p_{\mathrm{C}}$$

Effective pressure

Constitutive laws

Assumption/hypothesis to be tested

- We assume that the frozen part of the frozen clay is approximately transverse isotropic.
- We assume the isotropic plane is orthogonal to the largest temperature gradient component.

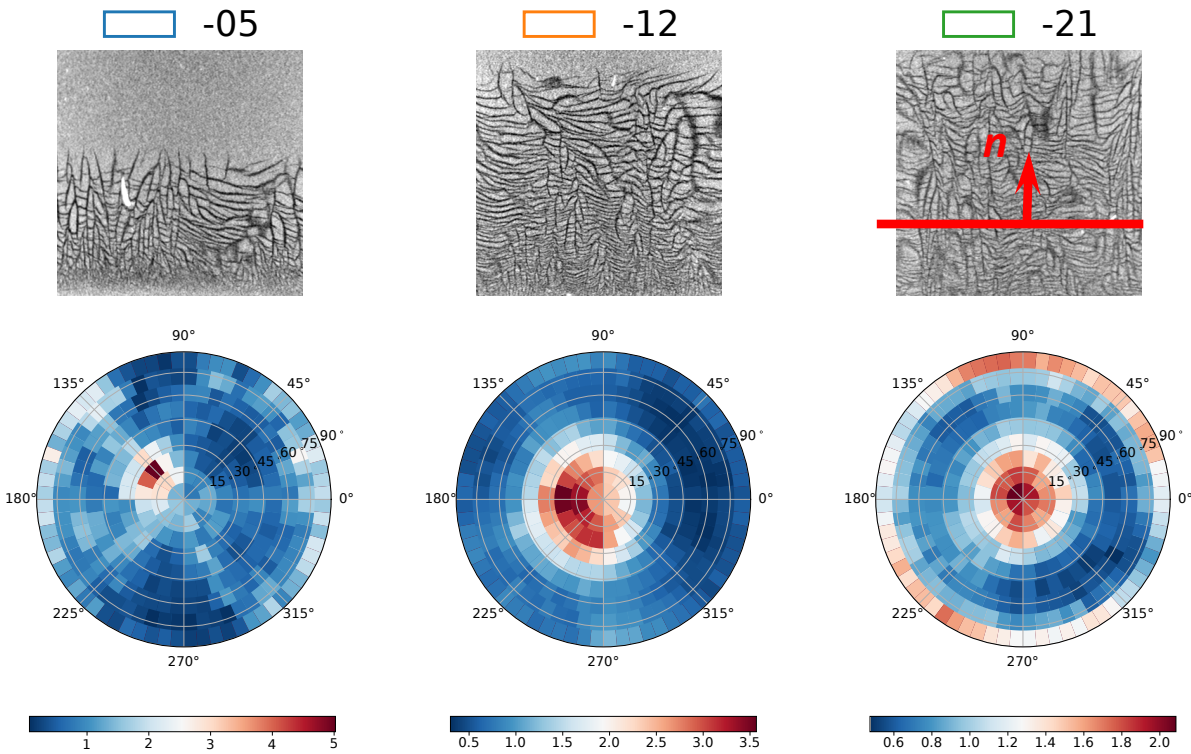

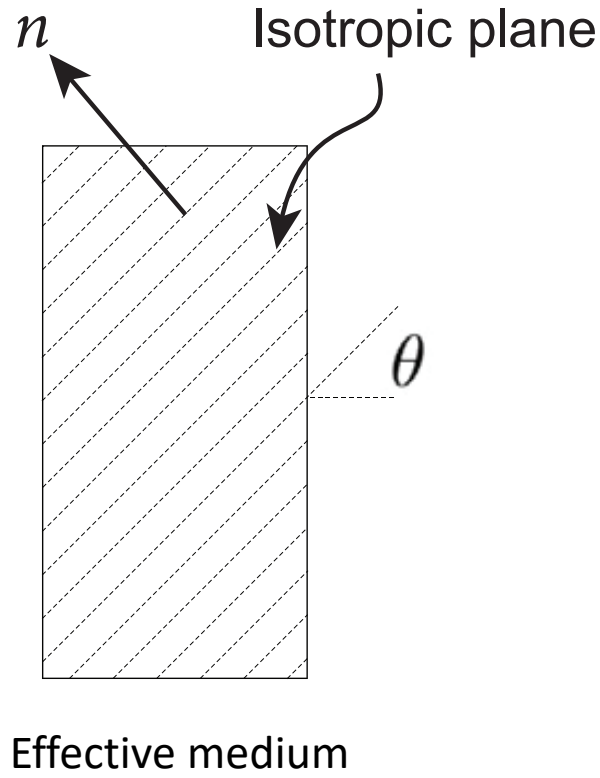

Anisotropic elasticity

- Consider the **isotropic** elastic stored energy function for soil. (Na and Sun 2017).

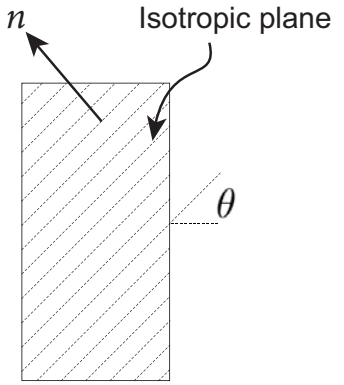

$$\Psi(\varepsilon_{\mathrm{v}}^{\mathrm{e}}, \varepsilon_{\mathrm{s}}^{\mathrm{e}}) = k s_{\mathrm{cryo}} \varepsilon_{\mathrm{v}}^{\mathrm{e}} - (p_0 - k s_{\mathrm{cryo}}) C_{\mathrm{r}} \exp\left(\frac{\varepsilon_{\mathrm{v}0} - \varepsilon_{\mathrm{v}}^{\mathrm{e}}}{C_{\mathrm{r}}}\right) + \frac{3}{2}\mu \varepsilon_{\mathrm{s}}^{\mathrm{e}2}$$

Cryo-suction pressure

- Projection of strain.

$$\boldsymbol{\varepsilon}^{\mathrm{e}*} = \mathbb{P} : \boldsymbol{\varepsilon}^{\mathrm{e}}$$

$$\mathbb{P} = c_1 \mathbb{I} + \frac{c_2}{2}(\boldsymbol{m} \oplus \boldsymbol{m} + \boldsymbol{m} \ominus \boldsymbol{m}) + \frac{c_3}{4}(\boldsymbol{I} \oplus \boldsymbol{m} + \boldsymbol{m} \oplus \boldsymbol{I} + \boldsymbol{I} \ominus \boldsymbol{m} + \boldsymbol{m} \ominus \boldsymbol{I})$$ (Semnani et al. 2018)

$$\boldsymbol{m} = \boldsymbol{n} \otimes \boldsymbol{n} \qquad (\bullet \oplus \circ)_{ijkl} = (\bullet)_{jl}(\circ)_{ik} \quad (\bullet \ominus \circ)_{ijkl} = (\bullet)_{il}(\circ)_{jk}$$

Anisotropic elasticity

- Freezing induced transverse isotropy

$$\mathbb{P} = c_1\mathbb{I} + \frac{c_2}{2}(\boldsymbol{m}\oplus\boldsymbol{m} + \boldsymbol{m}\ominus\boldsymbol{m}) + \frac{c_3}{4}(\boldsymbol{I}\oplus\boldsymbol{m} + \boldsymbol{m}\oplus\boldsymbol{I} + \boldsymbol{I}\ominus\boldsymbol{m} + \boldsymbol{m}\ominus\boldsymbol{I})$$

$$x = x(S_{\mathrm{C}}),\ \text{for } x = c_1, c_2, \text{and } c_3$$

Introduce freezing dependency

$$x = \exp(m_x S_{\mathrm{C}}^2 + n_x S_{\mathrm{C}}),\ \text{for } x = c_1, c_2, \text{and } c_3$$

- Elastic stored energy becomes:

$$\Psi(\varepsilon_{\mathrm{v}}^{\mathrm{e}*}, \varepsilon_{\mathrm{s}}^{\mathrm{e}*}) = ks_{\mathrm{cryo}}\varepsilon_{\mathrm{v}}^{\mathrm{e}*} - (p_0 - ks_{\mathrm{cryo}})C_{\mathrm{r}}\exp\left(\frac{\varepsilon_{\mathrm{v}0} - \varepsilon_{\mathrm{v}}^{\mathrm{e}*}}{C_{\mathrm{r}}}\right) + \frac{3}{2}\mu\varepsilon_s^{\mathrm{e}*2}$$

where

$$\varepsilon_{\mathrm{v}}^{\mathrm{e}*} = \mathrm{tr}(\boldsymbol{\varepsilon}^{\mathrm{e}*}) = (\mathbb{P} : \boldsymbol{I}) : \boldsymbol{\varepsilon}^{\mathrm{e}},\ \varepsilon_{\mathrm{s}}^{\mathrm{e}*} = \frac{\sqrt{2}}{3}\sqrt{\boldsymbol{\varepsilon}^{\mathrm{e}} : \mathbb{A}^* : \boldsymbol{\varepsilon}^{\mathrm{e}}},$$

$$\boldsymbol{\sigma}' = \frac{\partial\Psi}{\partial\boldsymbol{\varepsilon}^{\mathrm{e}}} = [ks_{\mathrm{cryo}} + (p_0 - ks_{\mathrm{cryo}})\exp\left(\frac{\varepsilon_{\mathrm{v}0} - \varepsilon_{\mathrm{v}}^{\mathrm{e}*}}{C_{\mathrm{r}}}\right)\left(1 + \frac{3\alpha\varepsilon_{\mathrm{s}}^{\mathrm{e}*2}}{2C_{\mathrm{r}}}\right)]\mathbb{P} : \boldsymbol{I} + \frac{2}{3}\mu\mathbb{A}^* : \boldsymbol{\varepsilon}^{\mathrm{e}},$$

More ice

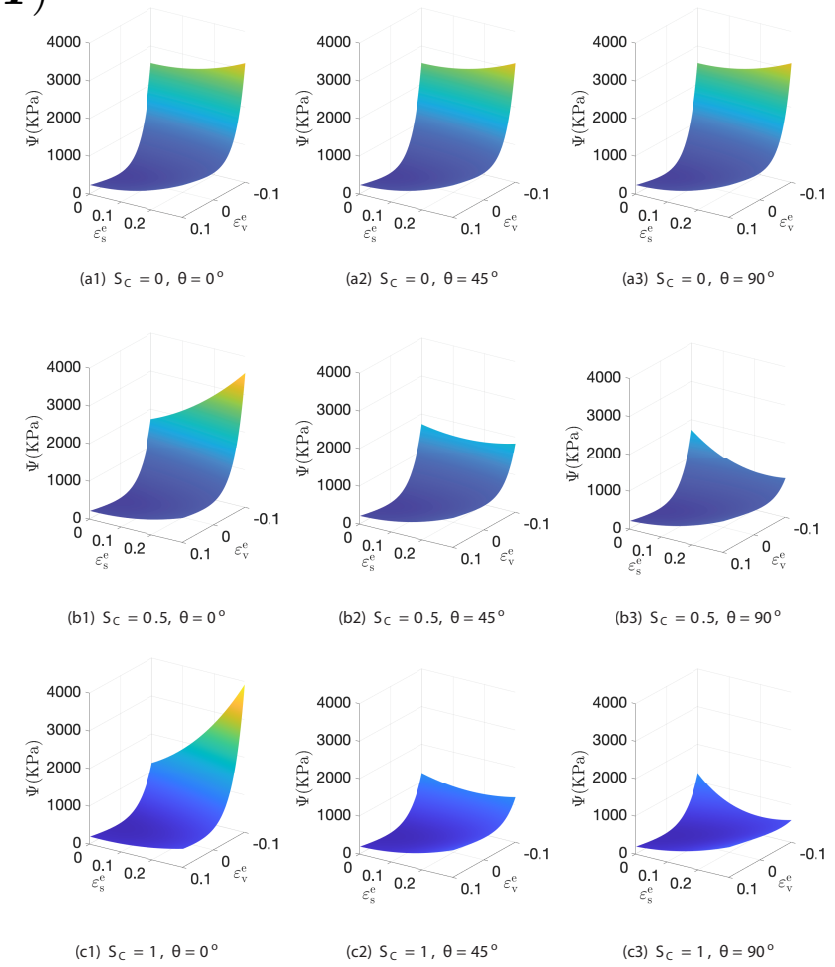

Anisotropic plasticity

- Consider Modified Cam-Clay yield criteria.
- Consider cryosuction effect (Nishimura et al. 2009).

$$f(p', q', p_c) = \frac{q'^2}{M^2} + \left(p' - \frac{p_c + k s_{cryo}}{2}\right)^2 - \left(\frac{p_c - k s_{cryo}}{2}\right)^2 \leq 0$$

Stress invariants

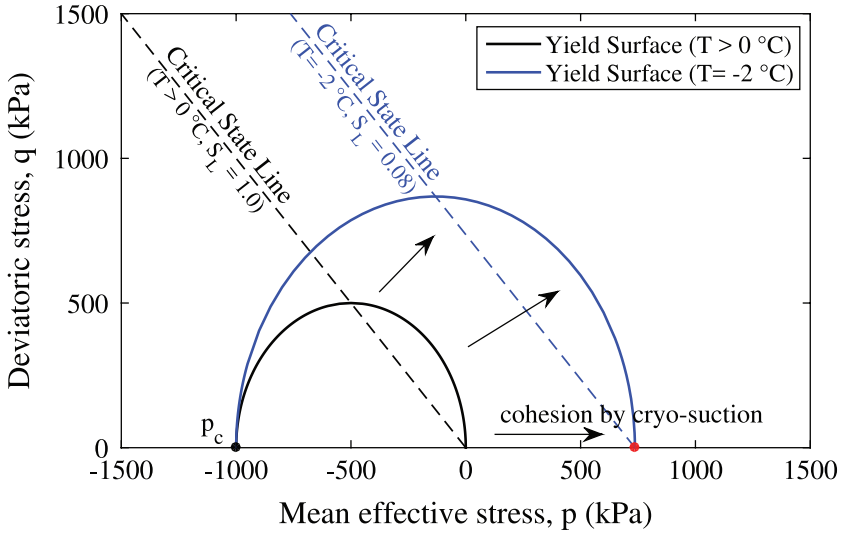

- Use the same projection tensor to project the stress. (Zhao et al. 2018)

$$\boldsymbol{\sigma'^*} = \mathbb{P} : \boldsymbol{\sigma'}$$

$$f(p'^*, q'^*, p_c) = \frac{q'^{*2}}{M^2} + \left(p'^* - \frac{p_c + k s_{cryo}}{2}\right)^2 - \left(\frac{p_c - k s_{cryo}}{2}\right)^2 \leq 0$$

$$\dot{p}_c = -\frac{\dot{\varepsilon}_v^p}{C_c - C_r} p_c$$

Freezing retention curves

- The objective of the model is to link the degree of liquid saturation with liquid pressure and temperature (similar to the three-phase characteristic curve for water-air-solid).
- Thermodynamic equilibrium of freezing soil (Clausius-Clapeyron equation, Nishmura et al., 2009)

$$p_{\mathrm{C}} = \frac{\rho_{\mathrm{C}}}{\rho_{\mathrm{L}}} p_{\mathrm{L}} - \rho_{\mathrm{C}} l \ln\left(\frac{T}{273.15}\right)$$

- Freezing characteristic function based on the van Genuchten (1980) model

$$S_{\mathrm{L}} = \left[1 + \left(\frac{s_{\mathrm{cryo}}}{P}\right)^{n}\right]^{-m}, \quad s_{\mathrm{cryo}} = \max(p_{\mathrm{C}} - p_{\mathrm{L}}, 0)$$

$$k_r = \sqrt{S_{\mathrm{L}}}\left[1 - \left(1 - S_{\mathrm{L}}^{1/m}\right)^{m}\right]^{2}$$

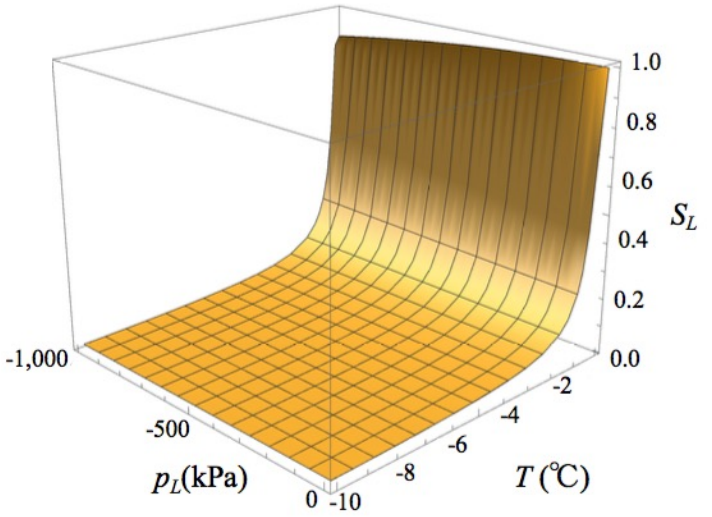

Degree of saturation

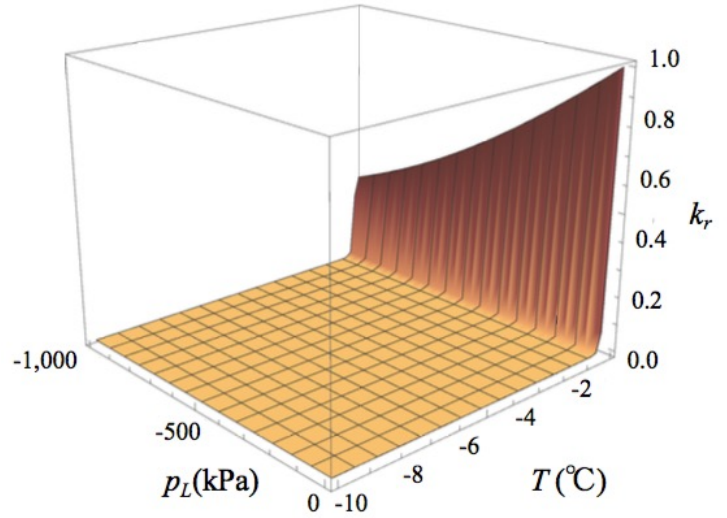

Relative Permeability

Numerical examples

- Boundary conditions.
- Compare isotropic and transversely isotropic models.
- Calibrate against experimental results: top displacement, lateral displacement, and freezing front.
  - Multi-objective optimization using Dakota software.

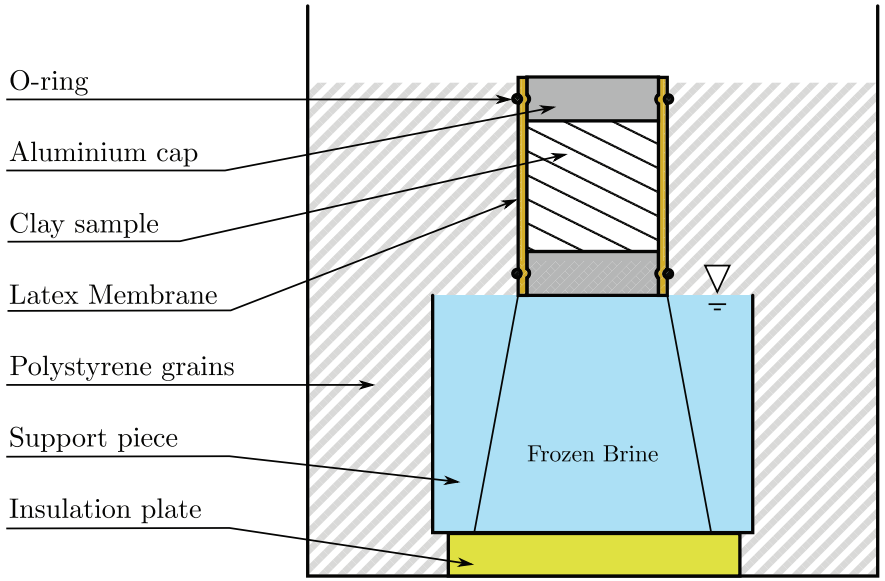

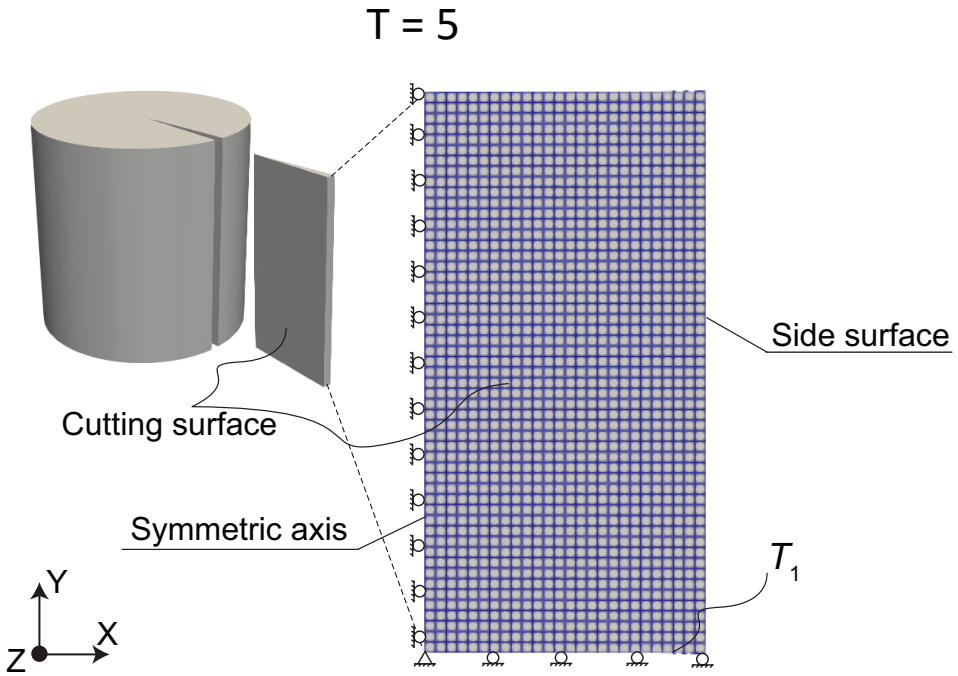

Results: Ice growth

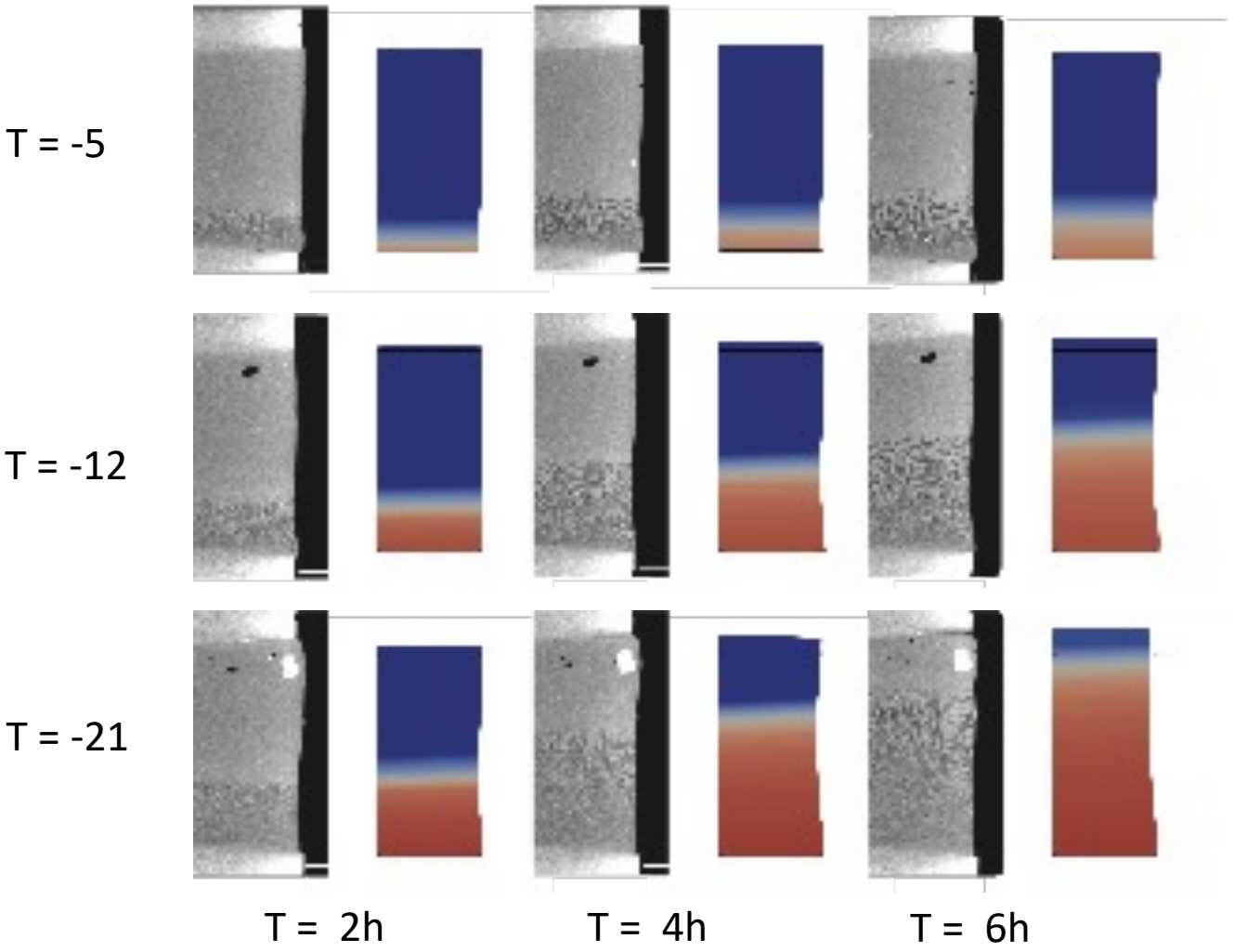

Results: Vertical displacement

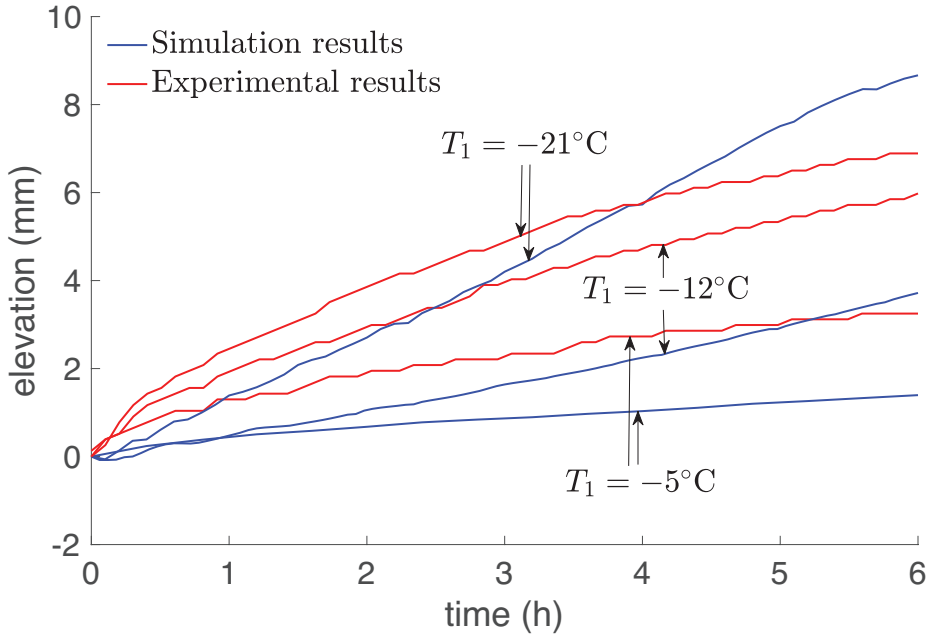

Transversely isotropic Model

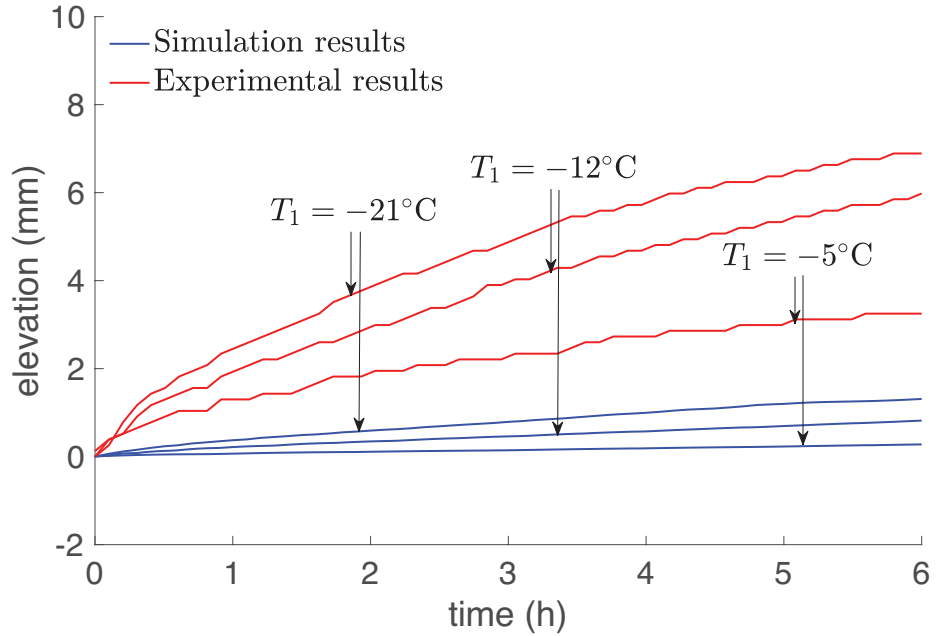

Isotropic benchmark

Results: Lateral displacement

Isotropic THM

Experiment

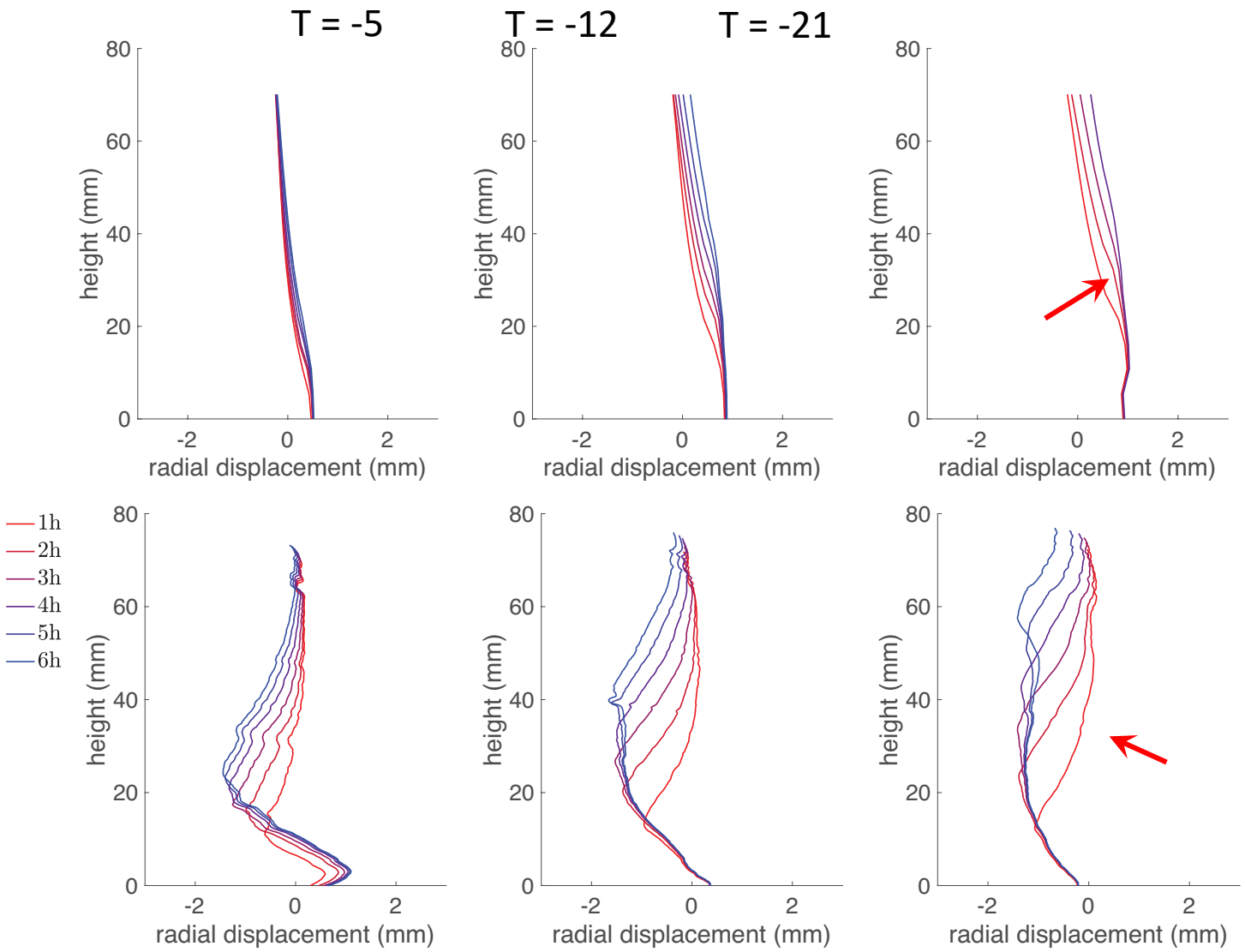

The prediction on the lateral deformation profile is wrong due to the isotropic assumption.

Results: Lateral displacement

T = -5 T = -12 T = -21

Freezing-dependent/Transversely isotropic

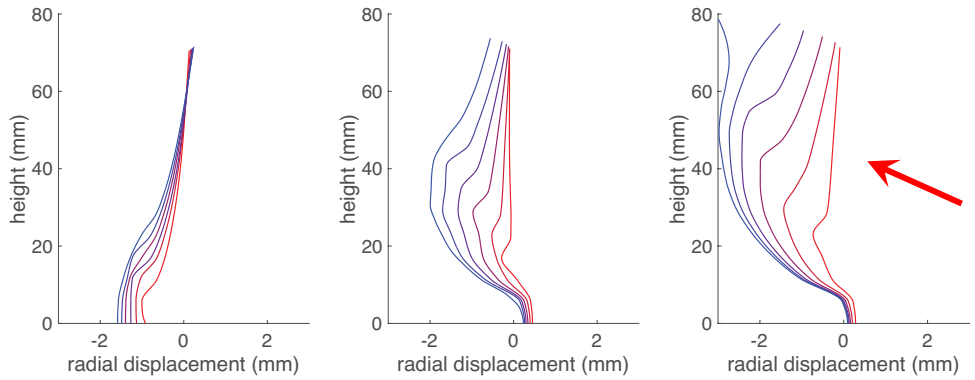

Experiment

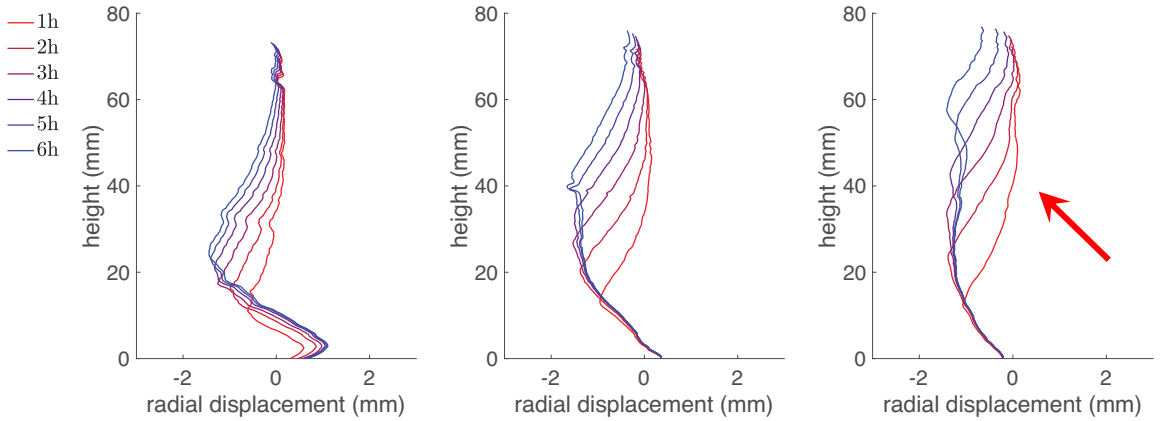

The predictions on the lateral expansion/contraction improve but not yet a perfect match.

Yin, Q., Andò, E., Viggiani, G., & Sun, W. (2022). Freezing-induced stiffness and strength anisotropy in freezing clayey soil: Theory, numerical modeling, and experimental validation. *International Journal for Numerical and Analytical Methods in Geomechanics*. 1– 28. https://doi.org/10.1002/nag.3380. (Cover)

Climate-controlled triaxial compression test on frozen Nevada sand

(a) Temperature = 25°C, quasi-static **(b)** Temperature = −1°C, strain rate = 10^{-6}/s **(c)** Temperature = −3°C, strain rate = 10^{-8}/s **(d)** Temperature = −3°C, strain rate = 10^{-8}/s

Colder

Climate-controlled biaxial compression simulation on frozen Oslo Clay

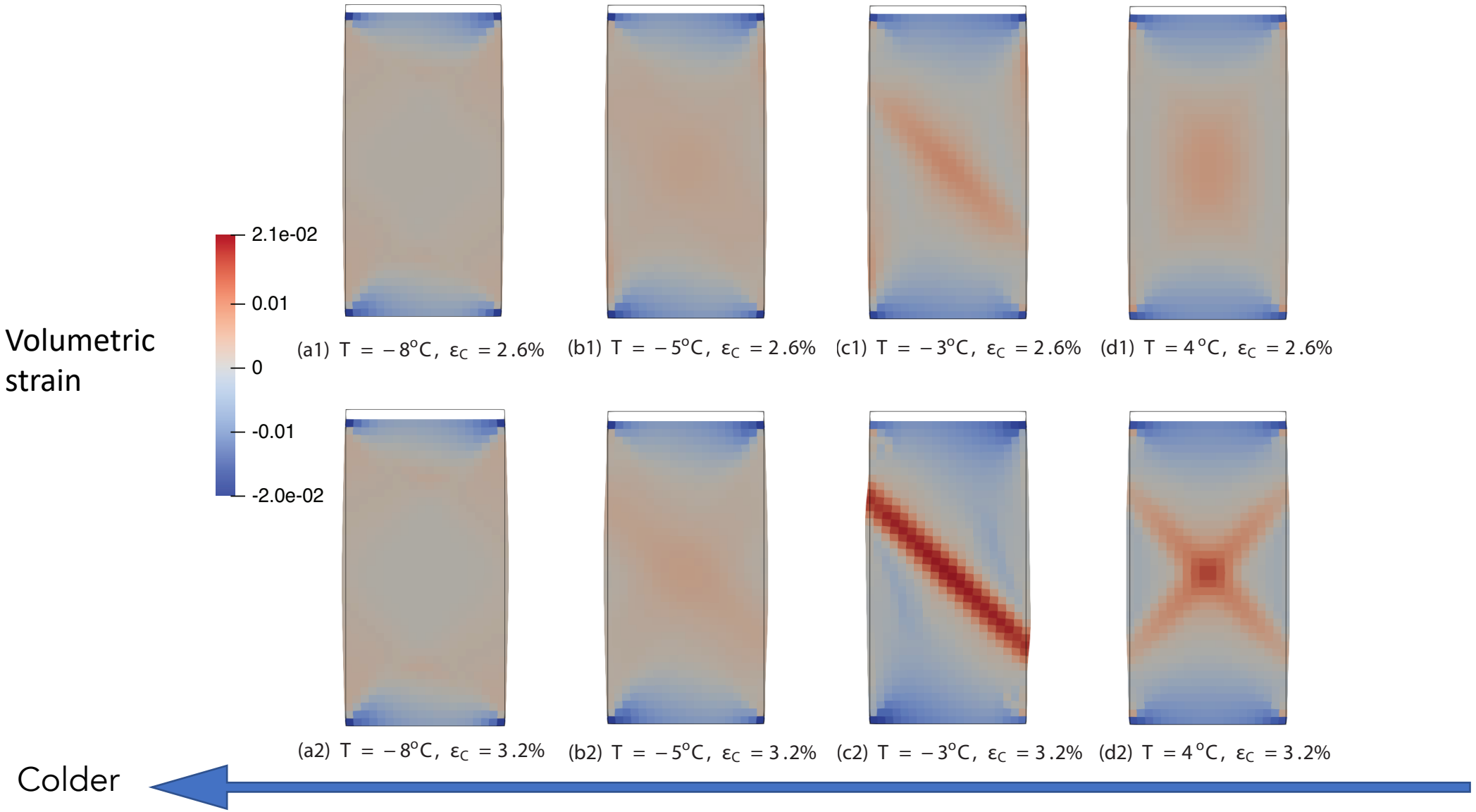

Climate-controlled biaxial compression simulation on frozen Oslo Clay

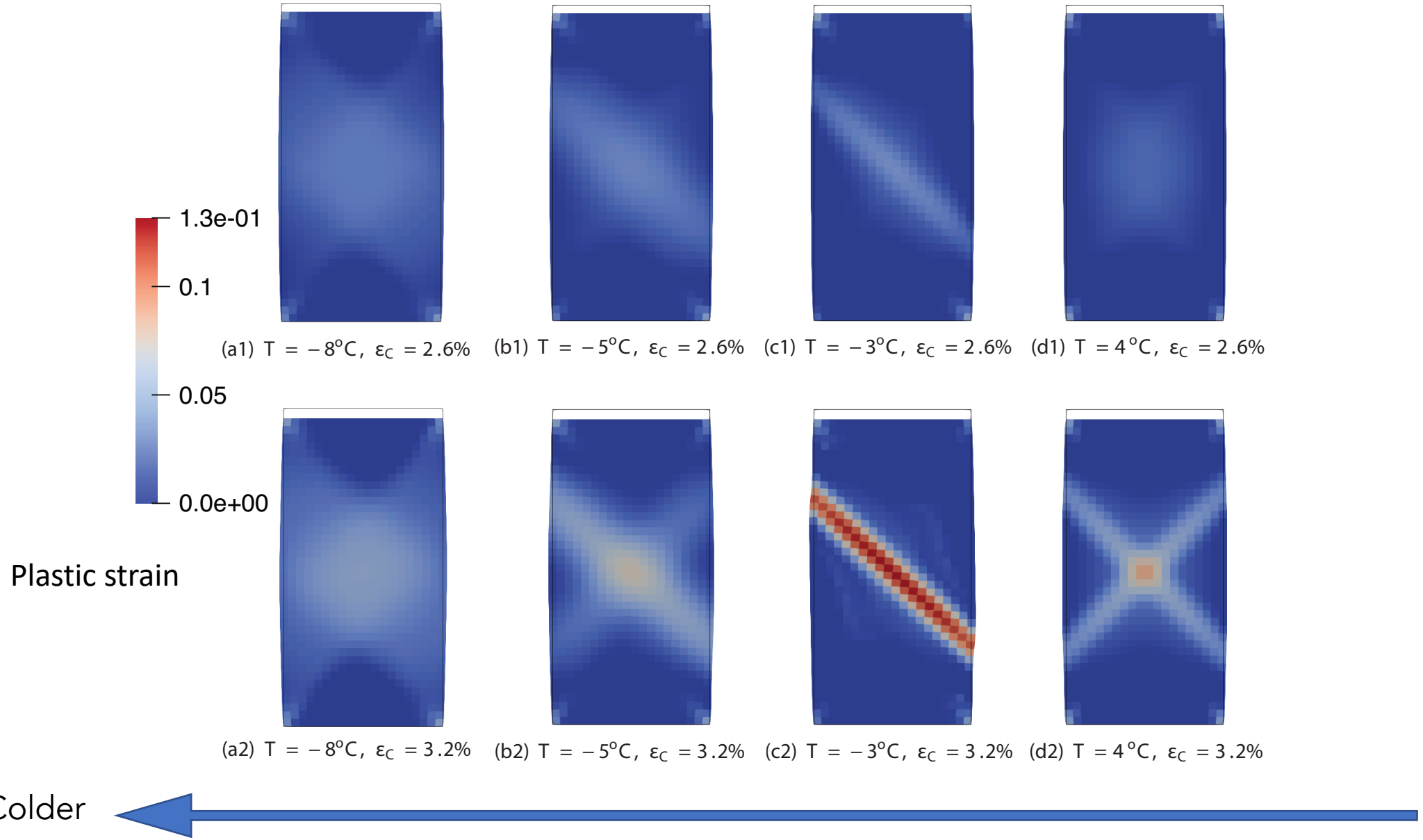

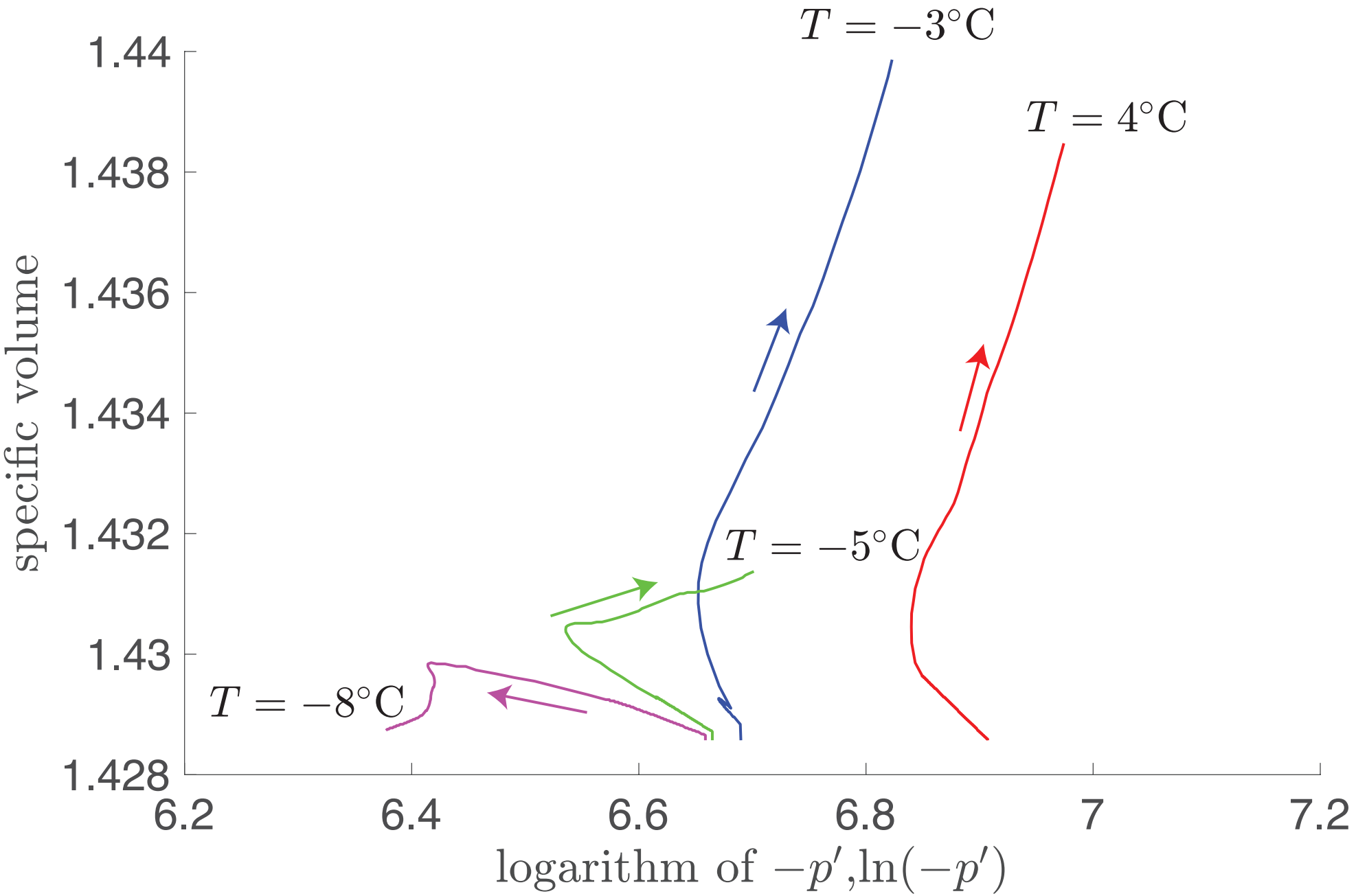
$T = -3°\mathrm{C}$
$T = 4°\mathrm{C}$
$T = -5°\mathrm{C}$
$T = -8°\mathrm{C}$
1.44
1.438
1.436
1.434
1.432
1.43
1.428
specific volume
6.2
6.4
6.6
6.8
7
7.2
logarithm of $-p'$,$\ln(-p')$

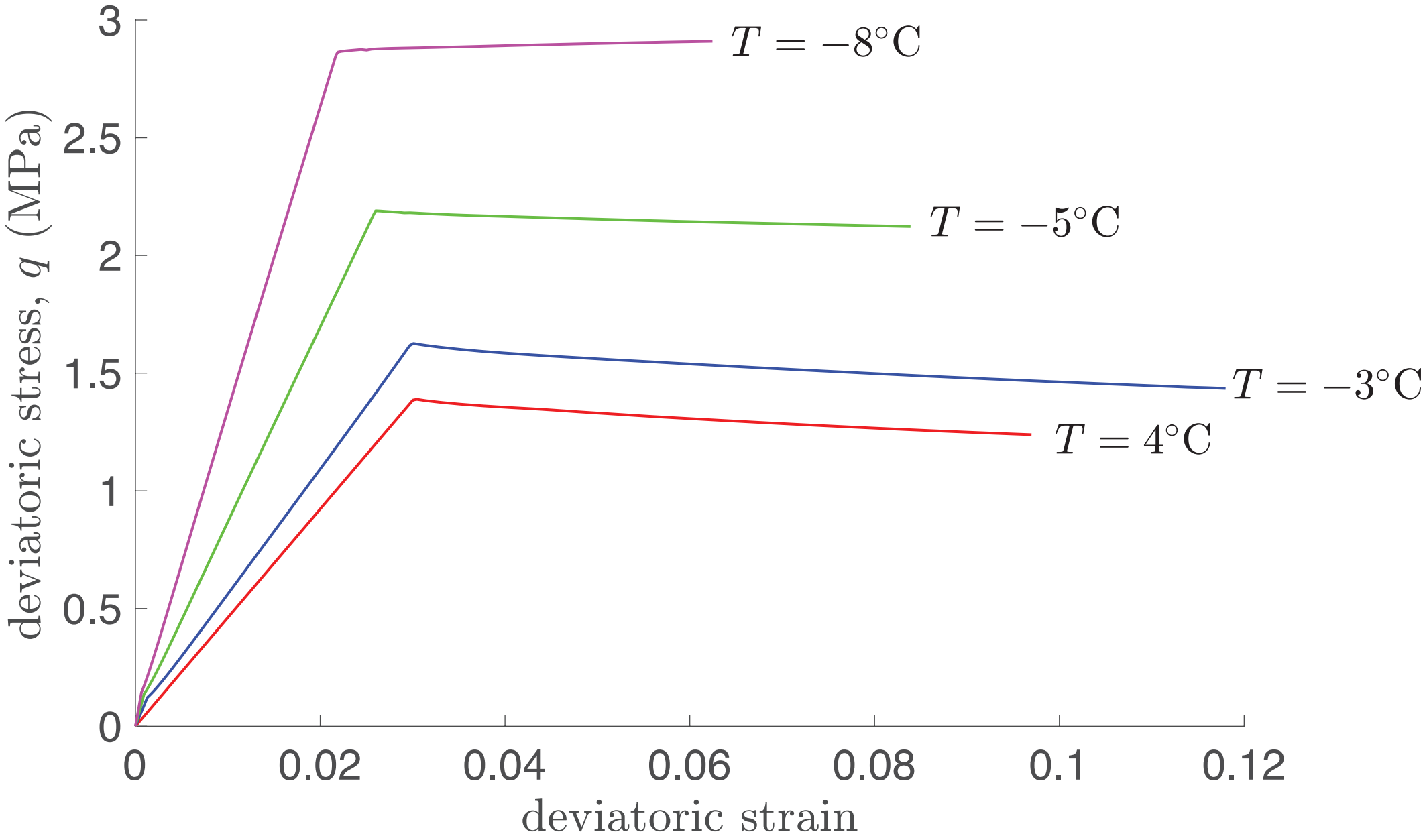
deviatoric stress, q (MPa)
3
2.5
2
1.5
1
0.5
0
0
0.02
0.04
0.06
0.08
0.1
0.12
deviatoric strain
$T = -8°\mathrm{C}$
$T = -5°\mathrm{C}$
$T = -3°\mathrm{C}$
$T = 4°\mathrm{C}$

Modeling the growth of of ice lens

Motivation

▶ Ice lensing and its consequences

- In the U.S., **~$2,000,000,000 had been spent annually** to repair frost damage of roads.
- Frost heaving and thawing settlement that damages the infrastructure: mainly due to the growth and thaw of **ice lenses**.
- **Ice lens: a body of ice accumulated in a localized zone**.

https://dmr.nd.gov

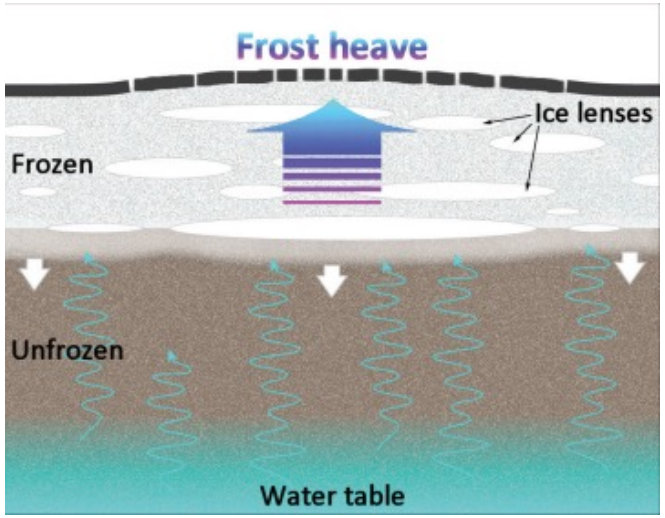

https://dmr.nd.gov

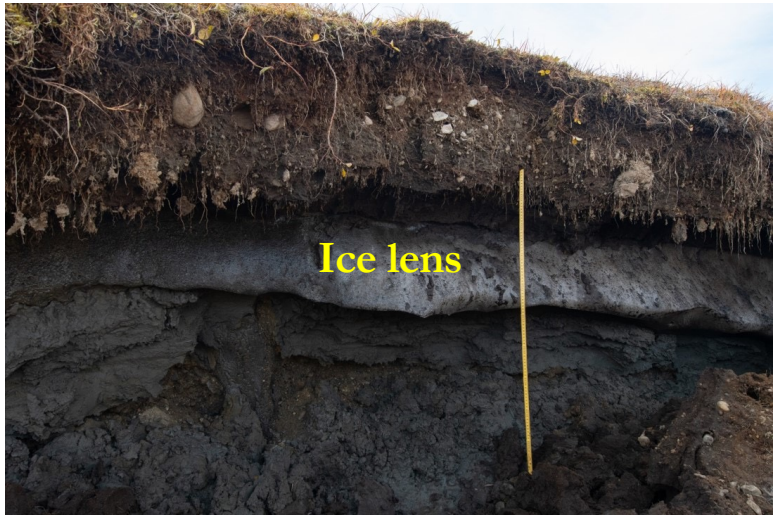

EGU BLOGS (https://blogs.egu.eu/)

▶ Miller's theory

- cf. Miller [1972], Miller [1977], Miller [1978], O'Neill and Miller [1985].
- A new ice lens can form if the **compressive effective stress** between particles is **zero or negative**.

→ *Ice lens can be viewed as* ***a segregated ice inside the freezing-induced fracture***.

Modeling approach

Frozen soil: three-phase material

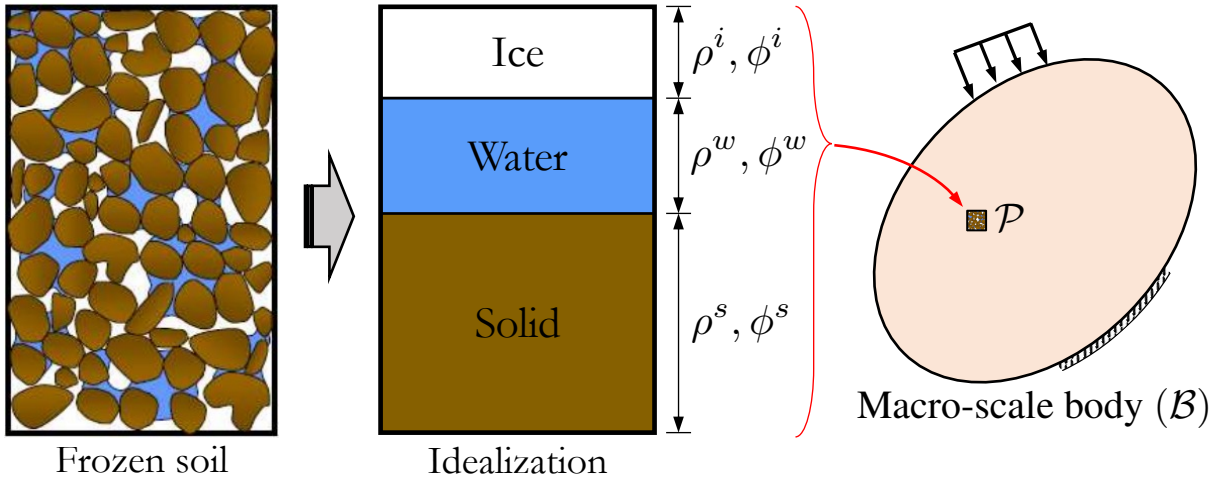

Modeling goal:

- Heat transport (Thermo-)
- Water migration towards the freezing front (Hydro-)
- Frost heave and thawing settlement (Mechanical)
- **Phase transition**
- **Brittle fracture**

Diffuse interface approximation via phase field

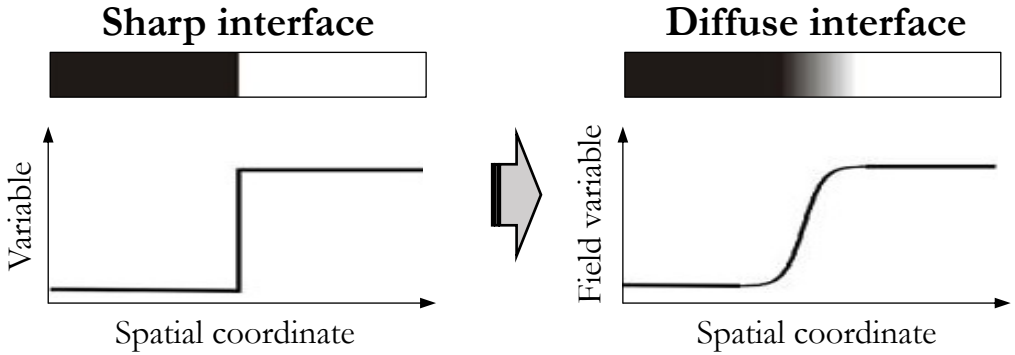

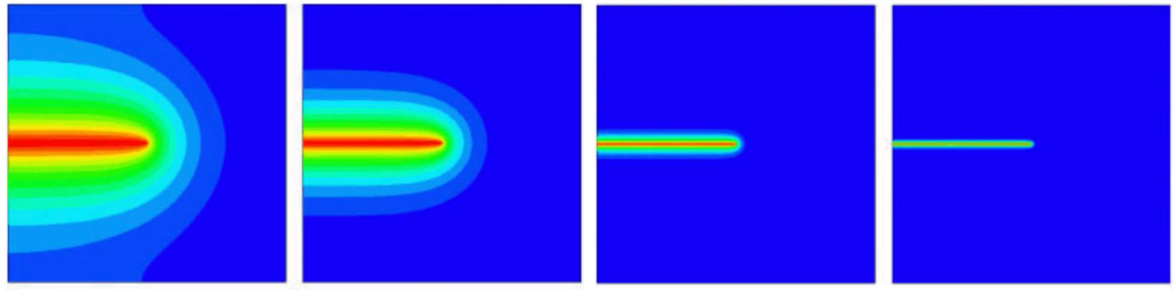

Reproduced from Miehe et al. [2010]

Modeling approach

▶ Multi-phase-field approach: ice lens

- **Ice lens** can be viewed as a segregated **ice** inside the freezing-induced **fracture**.

Phase field: c
- Indicates the **state of the fluid**.
- Solved via Allen-Cahn model:

$$-\frac{1}{M_c}\dot{c} = \frac{\partial f_c}{\partial c} - \epsilon_c^2 \nabla^2 c, \quad \text{where:} \begin{cases} c = 0 & : \text{frozen}, \\ c = 1 & : \text{unfrozen}, \\ c \in (0,1) & : \text{diffuse interface}, \end{cases}$$

Phase field: d
- Indicates the **damaged zone**.
- Phase field model for fracture:

$$-\frac{\partial g_d(d)}{\partial d}\mathcal{H}^* = d - l_d^2 \nabla^2 d, \quad \text{where:} \begin{cases} d = 0 & : \text{intact}, \\ d = 1 & : \text{damaged}, \\ d \in (0,1) & : \text{transition zone}, \end{cases}$$

$$\chi^i(c,d) = [1 - S^w(c)][1 - g_d(d)]$$

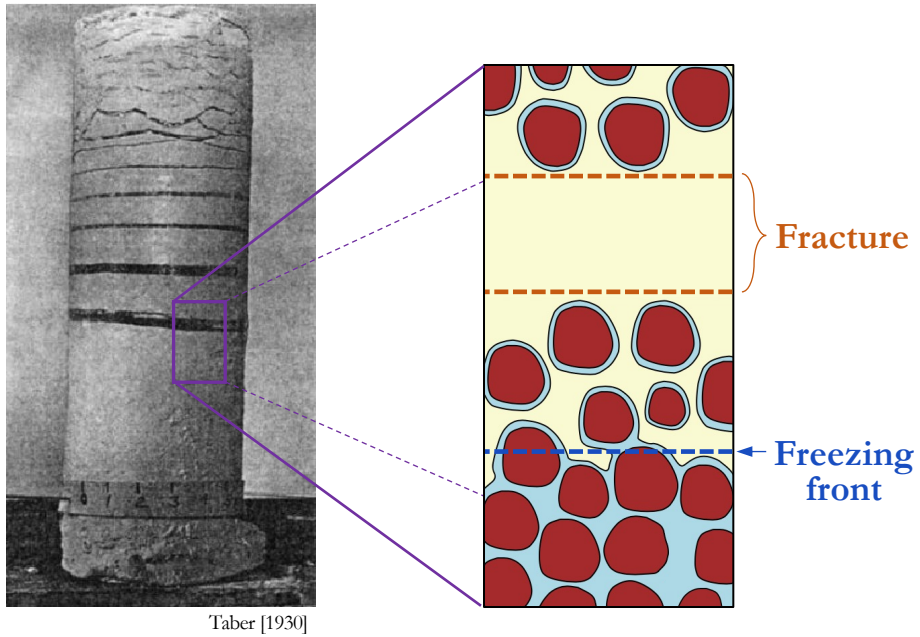

Taber [1930]

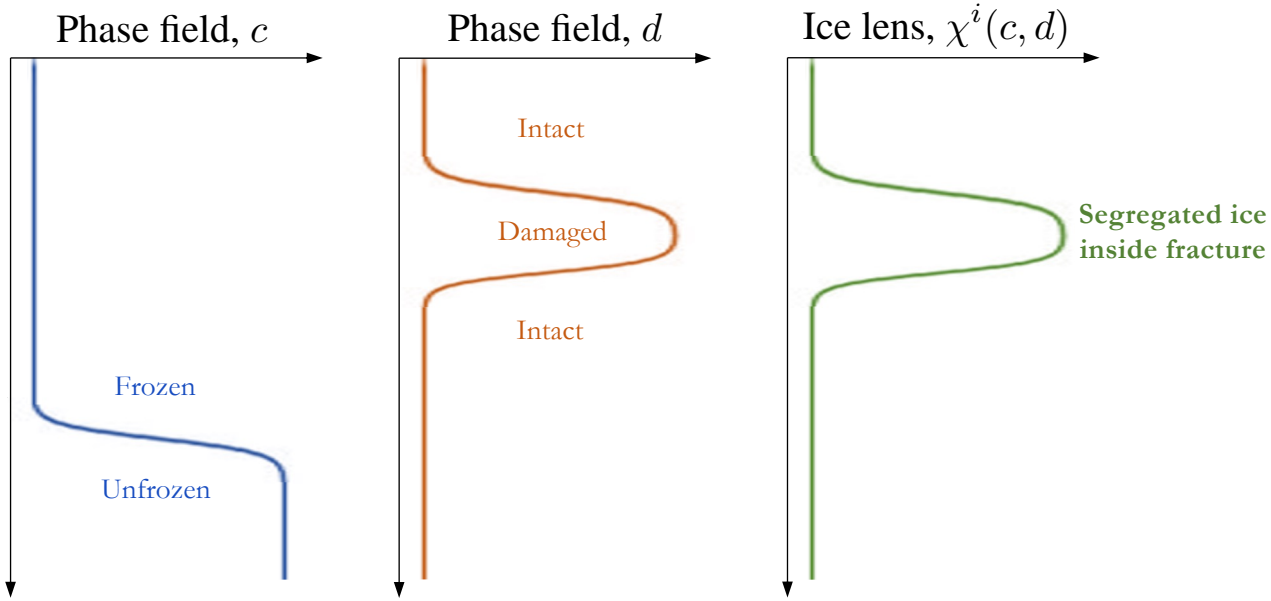

Modeling approach

▶ Effective stress principle

- Unlike crystallized ice inside the pores, deformation of ice lens induces the deviatoric stress:

$$\boldsymbol{\sigma} = \bar{\boldsymbol{\sigma}}' - \bar{p}\boldsymbol{I} - \phi[1 - S^w(c)]\bar{\alpha}_v K_i \boldsymbol{I}$$

Effective stress: $\bar{\boldsymbol{\sigma}}' = g_d(d)\bar{\boldsymbol{\sigma}}'_{\text{int}} + [1 - g_d(d)]\bar{\boldsymbol{\sigma}}'_{\text{dam}}$

- $\bar{\boldsymbol{\sigma}}'_{\text{int}}$: contribution from the solid skeleton
- $\bar{\boldsymbol{\sigma}}'_{\text{dam}}$: contribution from the ice lens

Pore pressure: $\bar{p} = S^w(c)p_w + [1 - S^w(c)]p_i$

- p_w : pore water pressure
- p_i : pore ice pressure

Volumetric expansion: $\bar{\alpha}_v = g_d(d)\bar{\alpha}_{v,\text{int}} + [1 - g_d(d)]\bar{\alpha}_{v,\text{dam}}$

- $\bar{\alpha}_{v,\text{int}}$: expansion coefficient (pore ice)
- $\bar{\alpha}_{v,\text{dam}}$: expansion coefficient (ice lens)

▶ Freezing retention and relative permeability

- Freezing retention curve: describes temperature-dependent cryo-suction.

$$s_{\text{cryo}} = p_i - p_w = p_{\text{ref}} \left\{ [\{\exp(b_B \langle \theta - \theta_m \rangle_-)\}]^{-\frac{1}{m_{vG}}} - 1 \right\}^{\frac{1}{n_{vG}}}$$ (van Genuchten [1980], DuWayne and Allen [1972])

- Relative permeability: describes the pore blocking due to in-pore crystallization of the ice phase.

$$\boldsymbol{w}_w = -\frac{k_r \boldsymbol{k}}{\mu_w}(\nabla p_w - \rho_w \boldsymbol{g}), \quad \text{where: } k_r = S^w(c)^{1/2} \left\{ 1 - \left[1 - S^w(c)^{1/m_{vG}} \right]^{m_{vG}} \right\}^2$$ (Luckner et al. [1989])

- $\boldsymbol{w}_w$: Darcy's velocity
- μ_w : water viscosity
- $\boldsymbol{k}$: permeability tensor
- k_r: relative permeability

$p_{\text{ref}}, m_{vG}, n_{vG}, b_B$: material parameters

Modeling approach

▶ Clausius-Clapeyron equation and Allen-Cahn model

- Phase field simulations for solidification (for pure substance):

$$\frac{1}{M_c}\dot{c} = \frac{\partial f_c}{\partial c} - \epsilon_c^2 \nabla^2 c, \text{ where the driving force: } f_c = W_c g_c(c) + \mathcal{F}_c(\theta) p_c(c), \quad \text{(Boettinger et al. [2002])}$$

while: $\boxed{\mathcal{F}_c(\theta) = \rho_i L_\theta \left(1 - \frac{\theta}{\theta_m}\right)}$ → **Clausius-Clapeyron eq.**

$\begin{cases} g_c(c) : \text{double-well potential} \\ p_c(c) : \text{interpolation function} \end{cases}$ $\begin{cases} W_c : \text{height of energy barrier} \\ M_c : \text{mobility parameter} \end{cases}$

- To replicate the intense growth of the ice lens, we replace $\mathcal{F}_c(\theta)$ with $\mathcal{F}_c^*(\theta, d)$,

$$\mathcal{F}_c^*(\theta, d) = \rho_i L_\theta \left(1 - \frac{\theta}{\theta_m}\right) + [1 - g_d(d)] K_c^* \left(1 - \frac{\theta}{\theta_m}\right)^{g_c^*}$$

K_c^*, g_c^* : kinetic parameters

Additional kinetic term that describes:
different growth rate between pore ice and ice lens.
(cf. Espinoza et al. [2008]; Choo and Sun [2018])

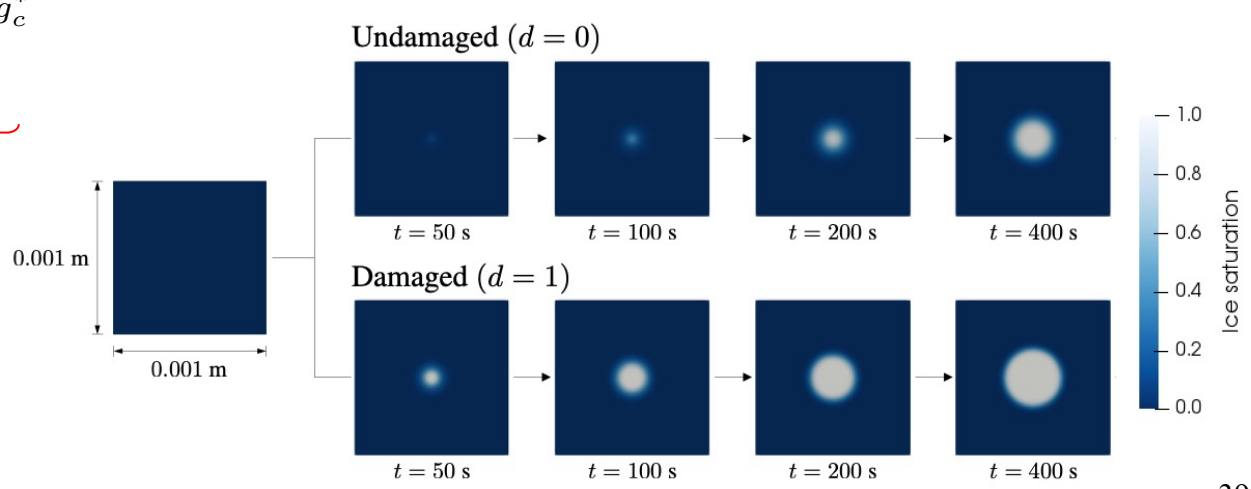

Multi-phase-field model for ice lens growth and thaw

▶ Governing field equations

- **Balance of linear momentum** (solid displacement, $\boldsymbol{u}$):

$$\nabla\cdot\boldsymbol{\sigma}+\rho\boldsymbol{g}=\boldsymbol{0}$$

- **Balance of mass** (pore water pressure, p_w):

$$\phi\dot{S}^w(c)(\rho_w-\rho_i)+\{S^w(c)\rho_w+[1-S^w(c)]\rho_i\}\nabla\cdot\boldsymbol{v}+\nabla\cdot\rho^w\tilde{\boldsymbol{v}}_w=0$$

- **Balance of energy** (temperature, θ):

$$(\rho^s c_s+\rho^w c_w+\rho^i c_i)\dot{\theta}+\phi\left[(\rho_w c_w-\rho_i c_i)(\theta-\theta_m)+\rho_i L_\theta\right]\dot{S}^w(c)+\nabla\cdot\boldsymbol{q}=\hat{r}$$

THM

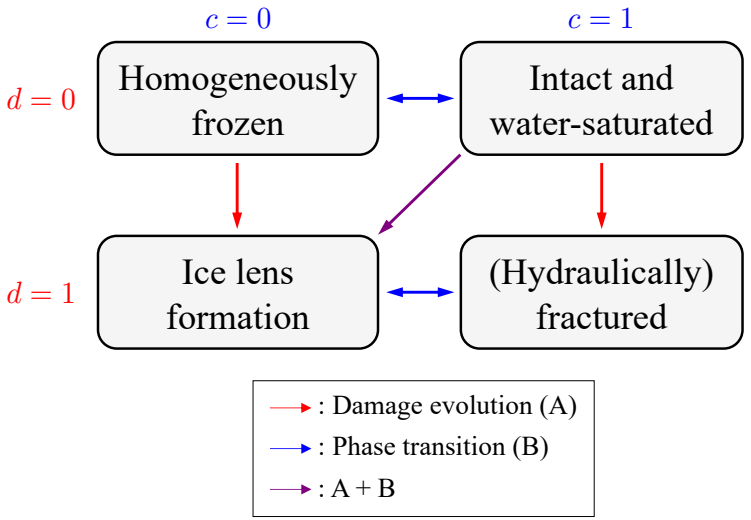

- **Damage evolution equation** (damage parameter, d):

$$\frac{\partial g_d(d)}{\partial d}\mathcal{H}^*+(d-l_d^2\nabla^2 d)=0$$

THM + Fracture

- **Allen-Cahn equation** (order parameter, c):

$$\frac{1}{M_c}\dot{c}+\frac{\partial f_c}{\partial c}-\epsilon_c^2\nabla^2 c=0$$

THM + Fracture + Phase transition

Numerical examples

▶ Validation exercise: homogeneous freezing

- Benchmark experiment by Feng et al. [2015].
- Unidirectional freezing (from the bottom to the top), unlimited water supply.
- Does not involve fracture process: homogeneous freezing.
- Temperature measurements: TC2, TC3, TC4.

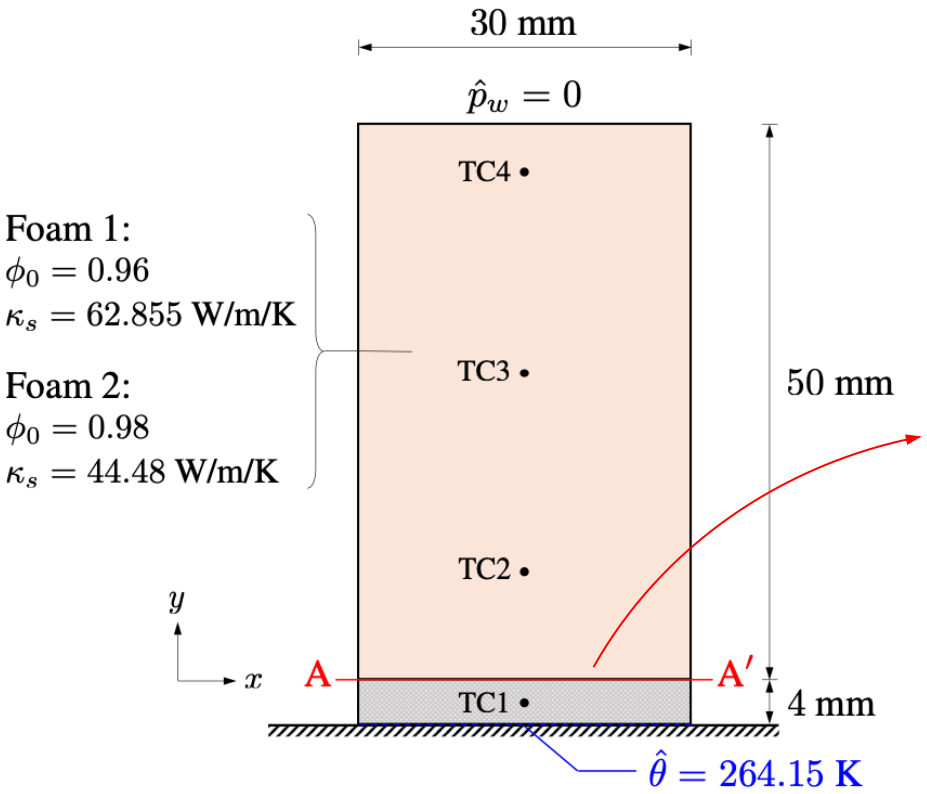

Numerical experiment

Directly applied temperature recorded at TC1 as a Dirichlet BC at plane AA'.

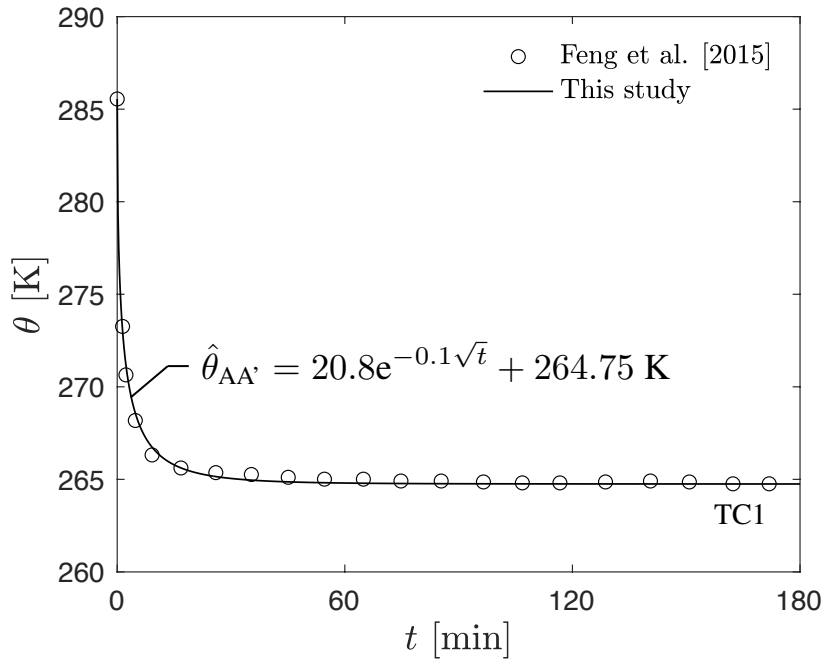

Numerical examples

▶ Validation exercise: homogeneous freezing

- Benchmark experiment by Feng et al. [2015].
- Unidirectional freezing (from the bottom to the top), unlimited water supply.
- Does not involve fracture process: homogeneous freezing.
- Temperature measurements: TC2, TC3, TC4.

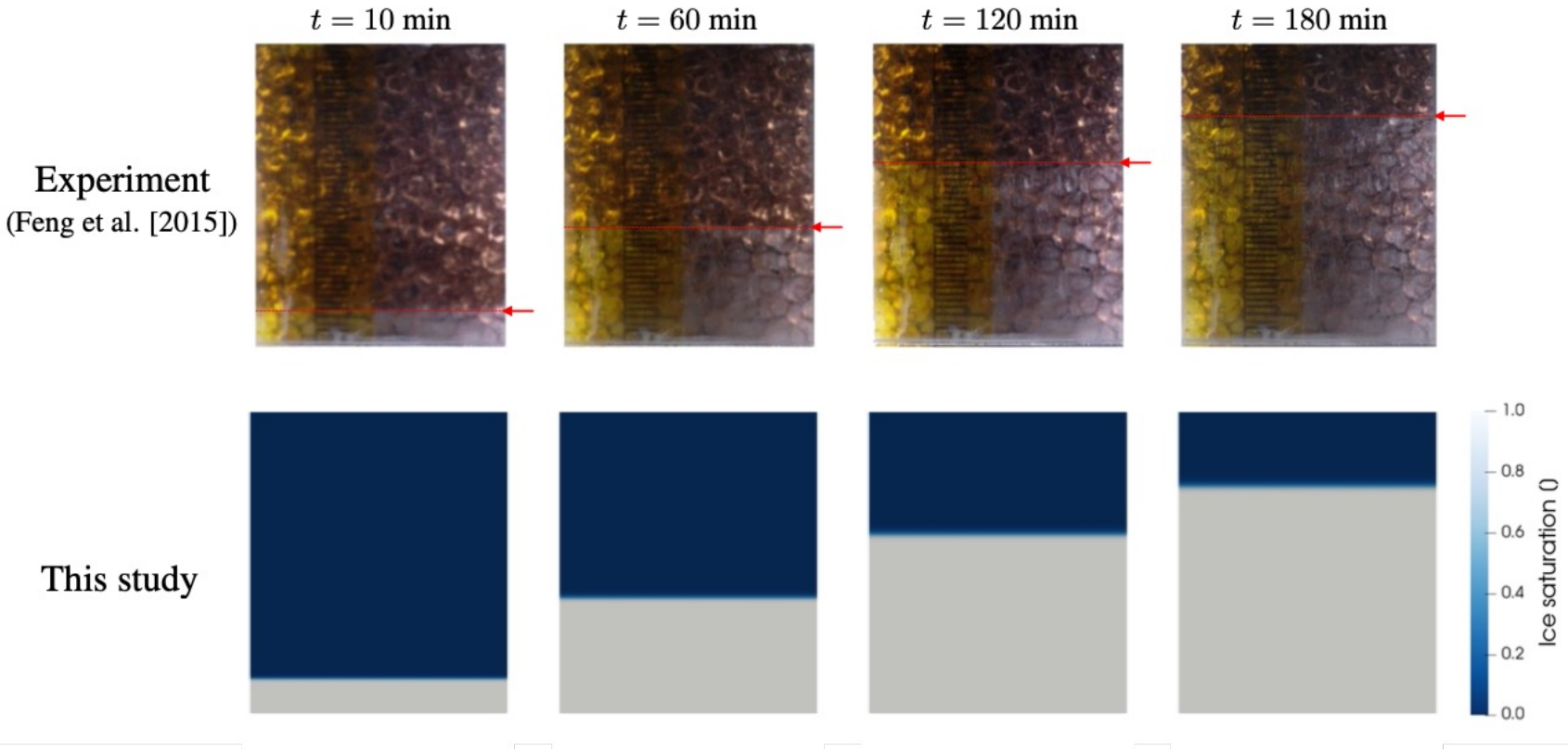

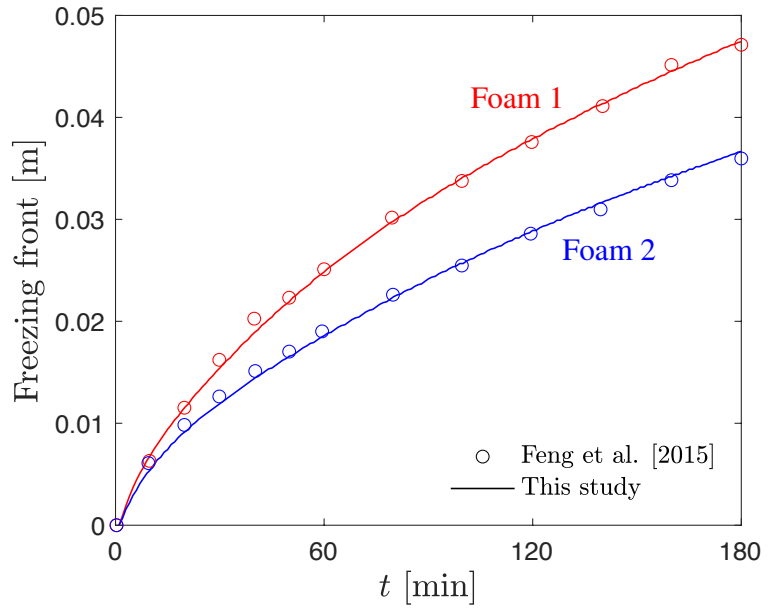

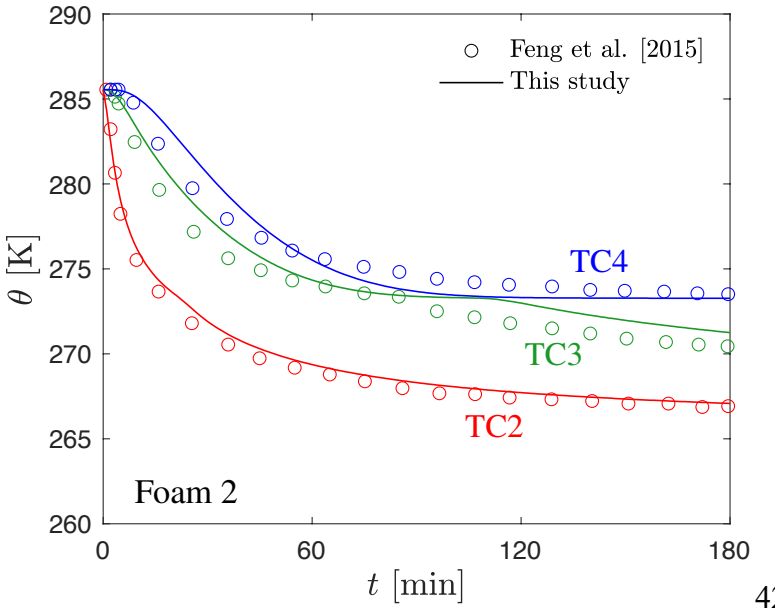

Numerical examples

▶ Multiple ice lens growth and thaw in heterogeneous soil

- Unidirectional freezing (from the top to the bottom), unlimited water supply.
- Random porosity profile, porosity-dependent material properties:

$$G = \frac{3}{2}\left(\frac{1-2\nu}{1+\nu}\right)\exp\left[10(1-\phi_0)\right] \quad \text{(Osman [2019])} \quad ; \qquad \mathcal{G}_d = \mathcal{G}_{d,\text{ref}}\left(\frac{1-\phi_0}{1-\phi_{\text{ref}}}\right)^{n_\phi} \quad \text{(Wang and Sun [2017])}$$

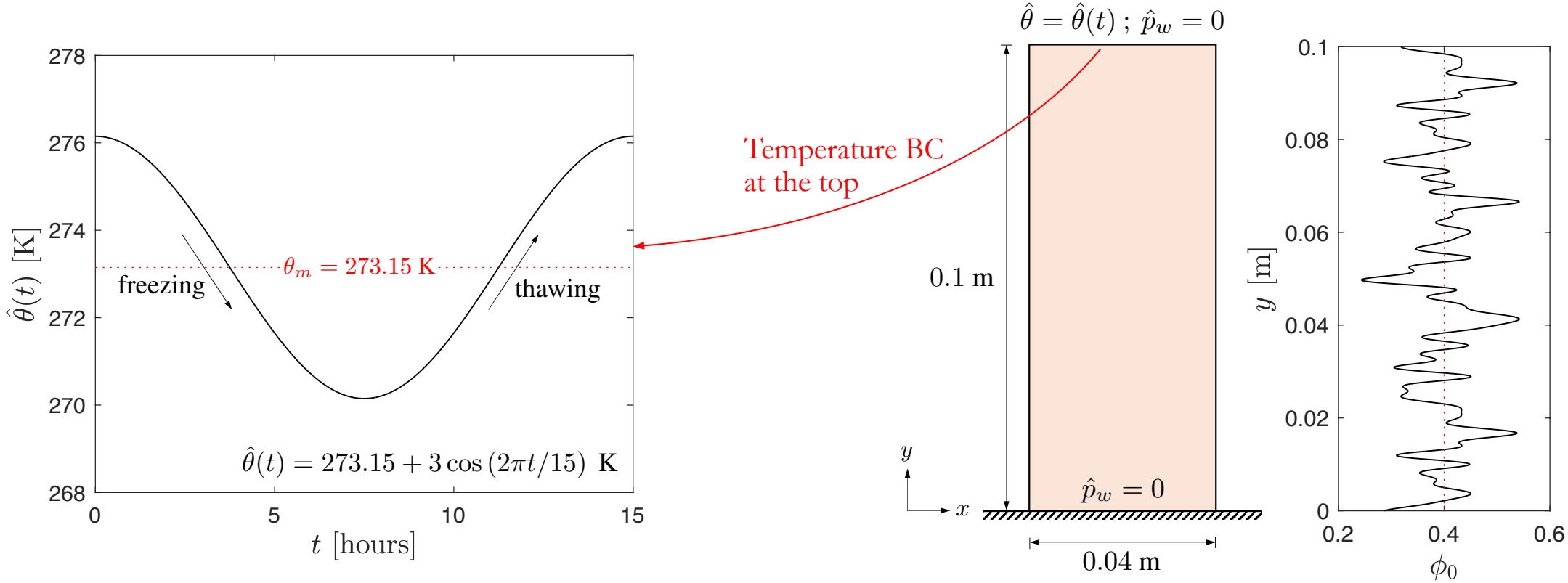

Numerical examples

▶ Multiple ice lens growth and thaw in heterogeneous soil

- Unidirectional freezing (from the top to the bottom), unlimited water supply.
- Random porosity profile, porosity-dependent material properties:

$$G = \frac{3}{2}\left(\frac{1-2\nu}{1+\nu}\right)\exp\left[10(1-\phi_0)\right] \quad \text{(Osman [2019])} \quad ; \qquad \mathcal{G}_d = \mathcal{G}_{d,\text{ref}}\left(\frac{1-\phi_0}{1-\phi_{\text{ref}}}\right)^{n_\phi} \quad \text{(Wang and Sun [2017])}$$

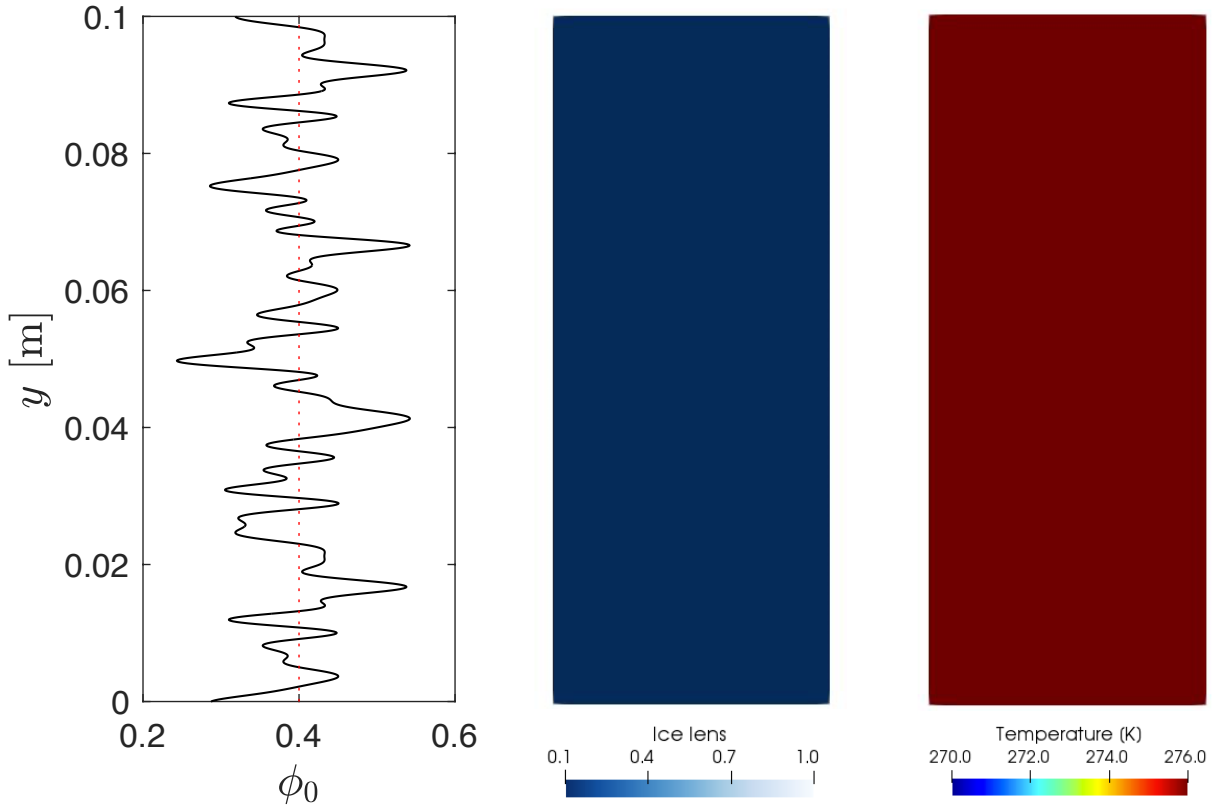

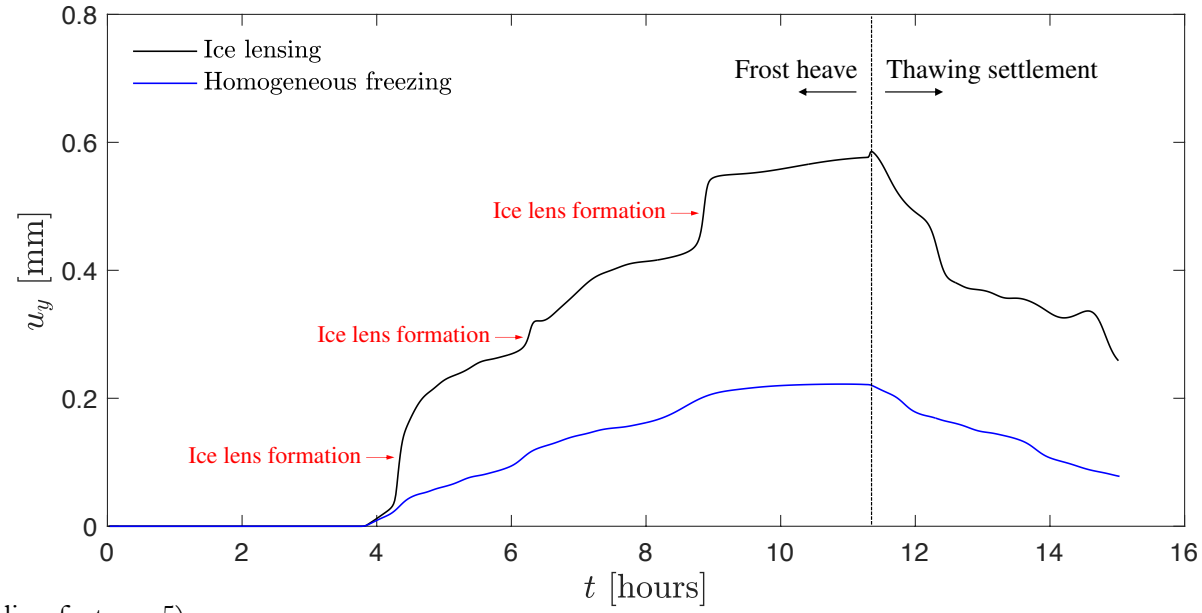

(scaling factor: x5)

Summary and conclusions

▶ Multi-phase-field approach for ice lens growth

- Ice lensing is modeled via combination of two phase fields (state variable and damage parameter) based on Miller's theory.

- Coupled with THM model, this approach can be viewed as a generalization of a model for phase-changing geomaterials.

▶ Freezing induced anisotropy for frozen soil

- We introduce an anisotropic critical state plasticity model for frozen soil.

- Compared with Micro-CT images obtained from a temperature gradient experiment, we found that the experiment results support the anisotropy hypothesis.

Further readings

International Journal for
Volume 46, No 11, 10 August 2022
Numerical and Analytical Methods in Geomechanics
Editors: F. Darve • R. de Borst • A. J. Whittle • R. I. Borja • G. Pijaudier-Cabot

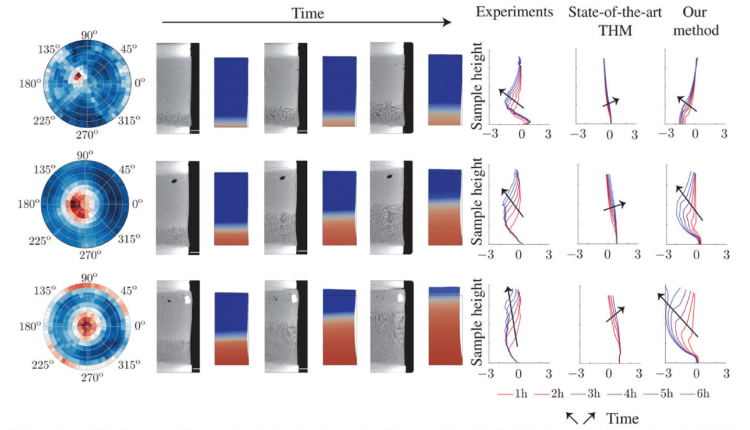

Orientations of ice lenses. Observed and simulated growth of ice in soil. Radial displacement (mm) along the height.

WILEY
ISSN 0363-9061
IJNGDZ 46(11) 1989–2208 (2022)

International Journal for
Volume 46, No 12, 25 August 2022
Numerical and Analytical Methods in Geomechanics
Editors: F. Darve • R. de Borst • A. J. Whittle • R. I. Borja • G. Pijaudier-Cabot

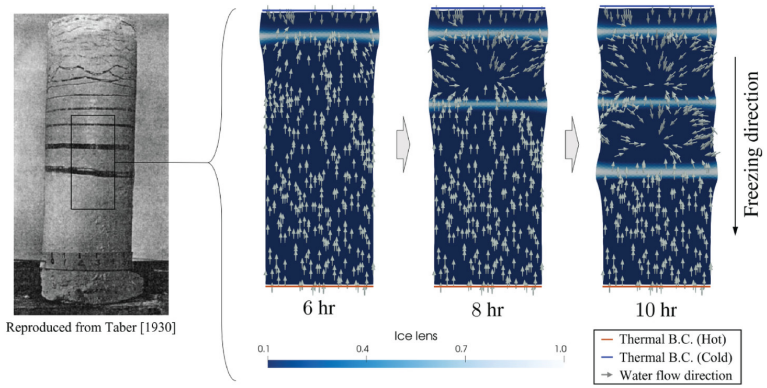

Reproduced from Taber [1930]

WILEY
ISSN 0363-9061
IJNGDZ 46(12) 2209–2412 (2022)

Acknowledgments

- Army Research Office
- US Department of Energy Office of Nuclear Energy

Thank You!

More information can be found at
www.poromehanics.org